AN EXPERIMENTAL DETERMINATION OF THE STRESS-STRAIN STRAIN RATE RELATIONS OF SEVERAL METALS

Thesis for the Degree of Ph. D.

MICHIGAN STATE UNIVERSITY

Ulric S. Lindholm

1960

THESIS

This is to certify that the

thesis entitled

AN EXPERIMENTAL DETERMINATION
OF THE STRESS-STRAIN STRAIN RATE RELATIONS
OF SEVERAL METALS

presented by

ULRIC S. LINDHOLM

has been accepted towards fulfillment
of the requirements for

DOCTOR OF PHILOSOPHY degree in APPLIED MECHANICS

Clement J. Lutes
Major professor

Date NOVEMBER 15, 1960

O-169

LIBRARY
Michigan State
University

ABSTRACT

In order to formulate an analytic solution to the problem of plastic wave propagation in metals more in formation on the rate dependence of the stress-strain relationship is necessary. In the present investigation stress-strain curves for three metals, lead, aluminum, and copper, were obtained over a range of strain rates from 10^{-4} in/in/sec to 10^{3} in/in/sec. These curves were all obtained at a nearly constant strain rate.

At the lower strain rates a universal testing machine was used. For the dynamic tests an adaptation of the method of Kolsky was employed where by short compression specimens were compressed between two sections of a split Hopkinson pressure bar. Loading was achieved by means of impact from a third striker bar which produced a long, flat-topped loading pulse. By means of strain gage pick-ups mounted on the pressure bars, a continuous record of the stress and strain in the specimen throughout the test could be obtained. Due to the nature of the loading pulse the elastic protion of the dynamic stress-strain curves could not be determined.

Over the entire range of strain rates covered the stress-strain curves for all three metals formed a homologous set with an increase in stress produced by an increase in the rate of straining for any given strain. The dependence of stress on the strain rate was found to follow the logarithmic law of Prandtl

$$\sigma = \sigma_o + k \log \dot{\epsilon} \ ,$$

when σ_o and k are functions of strain $\sigma_o(\epsilon)$ is the stress-strain curve at unit strain rate. $k(\epsilon)$ was found to be an increasing function of strain,

indicating that the tangent modulus also increased with an increase in strain rate. A measure of the rate sensitivity of a material is given by k/σ_o. Values of k, σ_o, and k/σ_o are given at several values of strain for lead, aluminum and copper.

AN EXPERIMENTAL DETERMINATION OF THE STRESS-STRAIN STRAIN RATE RELATIONS OF SEVERAL METALS

by

Ulric S. Lindholm

A THESIS

Submitted to the School of Advanced Graduate Studies

of Michigan State University of Agriculture and

Applied Science in partial fulfilment of

the requirements for the degree of

DOCTOR OF PHILOSOPHY

Department of Applied Mechanics

1960

Approved Clement A. Tatro

J 15166
6/19/61

ACKNOWLEDGEMENTS

I especially wish to express my gratitude to Dr. L. E. Malvern who originally suggested the problem and gave valuable advise throughout the project, and to Dr. C. A. Tatro for his continuous assistance in solving the experimental problems encountered and reading of the manuscript. I am also indebted to the other members of my committee, Dr. G. Mase and Dr. C. Wells.

Sincere thanks are also due to Mr. J. Hoffman and the Division of Engineering Research for their co-operation and support of this work.

I would also like to thank Mr. R. Jenkens and Mr. E. Thompson for their assistance in building the apparatus.

1. INTRODUCTION AND PURPOSE

In general stress may be thought of as a function of strain, strain rate, and temperature such that

$$\sigma = F(\epsilon, \dot{\epsilon}, T).$$

For usual engineering applications the temperature is assumed to be held within comparatively narrow bounds, and also the loads are taken to be applied "statically", where the effect of strain rate may be small. Thus, in these cases the stress is taken only as a function of the strain as indicated by the static stress-strain curve. It has long been realized, however, that the stress-strain curve is affected by varying the temperature and/or the rate of straining. Thus, there has been a considerable amount of work done and data obtained toward determining the magnitude of these effects. Stress-strain curves have been obtained in both the high and low temperature domains. Also the effect of strain rate from the static range down to creep or stress relaxation tests has come under considerable scrutiny. For very high strain rates, such as those that would come into effect in impact or wave propagation problems, however, there is considerably less definite information. This is due principally to the difficulty of the experimental problem of measuring stresses and strains when they are applied in very short periods of time. It is only in recent years that an attack on the problem has been made possible through the advent of electronic measuring and recording devices.

The purposes of this investigation then are to:

(1) Experimentally determine stress-strain curves for several metals at very high strain rates, these curves extending well into the

plastic range, with the tests to be conducted at constant (room) temperature.

(2) Correlate these stress-strain curves with curves at "slow" rates obtainable on a standard universal testing machine.

(3) Attempt to deduce a functional relationship between stress, strain, and strain rate at constant temperature.

2. HISTORICAL BACKGROUND

2.1. Interest In The Problem

The interest in stress-strain-strain rate effects has been from several points of view. First, from the influence of the rate of loading on the standard static tension or compression test, a factor which may be of considerable importance for many materials. Secondly, the recognition of the importance of impact loading and the development of impact tests, such as the Charpy or Izod tests, showed that the maximum stress and the energy absorbed by specimens subjected to impact were greater than in the case of static loading. Also stresses greatly exceeding the static yield stress could be sustained by materials without plastic deformation if the loads applied were of extremely short duration. These facts indicated that a different stress-strain relationship was needed to account for these phenomena. A third and comparatively recent interest in dynamic stress-strain relations has grown out of the development of the theory of plastic wave propagation. It is from this aspect of the problem that the present investigation was initiated.

An analytic solution to the plastic wave propagation problem was first obtained during World War II in this country by von Karman[1] and in England by Taylor[2] working independently. A principal conclusion of their analysis was that for a non-decreasing axial impact load each in-

crement of stress would be propagated at the velocity c such that

$$c = \sqrt{\frac{1}{\rho} \frac{d\sigma}{d\epsilon}} , \qquad (1)$$

where ρ is the density and $\frac{d\sigma}{d\epsilon}$ is the slope of the stress-strain curve at the given stress level. This relation had also been proposed earlier by Donnell[3]. It is seen that in the elastic region this reduced to the well known elastic wave velocity $c_o = \sqrt{E/\rho}$. The von Karman - Taylor theory assumed a unique stress-strain relation indpendent of the rate of strain. This relation was taken as the static stress-strain curve as dynamic relations were not known. Experimental verification of the theory[4] showed some deviations from the predicted behavior. These deviations indicated that a solution incorporating a strain rate effect would perhaps be more accurate.

Such a solution was obtained in 1951 by Malvern[5]. Malvern assumed that the stress could be taken as a function of the plastic strain ϵ_p and the plastic strain rate $\dot{\epsilon}_p$, such that

$$\sigma = \phi (\epsilon_p, \dot{\epsilon}_p)$$

If this is solved for $\dot{\epsilon}_p$, we get

$$\dot{\epsilon}_p = g (\sigma, \epsilon) \qquad (2)$$

and by including the elastic portion of the strain

$$\frac{\partial \epsilon}{\partial t} = \frac{1}{E} \frac{\partial \sigma}{\partial t} + g (\sigma, \epsilon) \qquad (3)$$

where E is the modulus of elasticity and $g(\sigma,\epsilon)$ is an assumed or experimentally determined function of the stress and strain. Malvern conjectured that the function $g(\sigma,\epsilon)$ should be a function of $\sigma - f(\epsilon)$, where $\sigma = f(\epsilon)$ represents a quasi-static or equilibrium stress-strain relation, i.e., one that is independent of time effects. Thus flow was assumed to occur only when $\sigma \geq f(\epsilon)$ and the plastic strain rate would be a function only of the excess of instantaneous stress σ over the equilibrium stress at the corresponding strain. It may be noted that this type of relation will only be valid for cases of short time or impact loading, because a true equilibrium or strain rate independent stress-strain relationship is not feasable due to creep effects. Due to the lack of experimental evidence and the need to make the mathematical problem tractable, the function $g(\sigma, \epsilon)$ was simplified to be linearly proportional to $\sigma - f(\epsilon)$. Thus, Equations (2) and (3) become

$$\dot{\epsilon}_p = k[\sigma - f(\epsilon)] \tag{2a}$$

and

$$\frac{\partial \epsilon}{\partial t} = \frac{1}{E}\frac{\partial \sigma}{\partial t} + k[\sigma - f(\epsilon)] \tag{3a}$$

One conclusion from this strain rate dependent theory is that the leading wave front of each increment of plastic stress will travel at the elastic wave speed and not according to Equation (1) as predicted by the rate independent theory. This conclusion was later verified experimentally by Sternglass and Stuart[6] who showed that for a material prestressed into the plastic range, a small additional increment of impact stress

would be propagated at the elastic velocity, not at the velocity determined from the slope of the stress-strain curve at the prestress level. Other differences from the strain rate independent theory need further experimental verification.

Other relations than the linear strain rate dependence of Malvern have been proposed. Prandtl[7] on theoretical grounds derived a relationship of the form

$$\dot{\epsilon}_p = A\, e^{B\sigma},$$

where A and B are constants. Again including the elastic strain this gives

$$\frac{\partial \epsilon}{\partial t} = \frac{1}{E}\frac{\partial \sigma}{\partial t} + A\, e^{B\sigma}.$$

Previously Ludwik[8] and later Deutler[9] added experimental support to this form.

Some experimental evidence[10] has also shown that a better fit to the data may be obtained by taking

$$\sigma = A\, \dot{\epsilon}^{n},$$

where A and n are again constants.

To compare these three proposed forms of strain rate dependence let us write them in the form

$$\sigma = \sigma_o + k_1 \dot{\epsilon} \qquad (4)$$

$$\sigma = \sigma_o + k_2 \ln \dot{\epsilon} \tag{5}$$

$$\sigma = \sigma_o \dot{\epsilon}^n \tag{6}$$

Here we are assuming that the plastic deformations are large and the elastic components of the strain may be neglected. In Equation (4), σ_o represents the equilibrium stress, i.e., the stress at which $\dot{\epsilon}$ is taken as zero. In Equations (5) and (6), σ_o is the stress corresponding to unit strain rate. σ_o, k_1, k_2 and n may in general be functions of the strain ϵ. These three relations will be referred to as the linear, logarithmic, and exponential strain rate laws respectively.

2.2 History Of Experimental Techniques

Experimental verification of the above relations for strain rate dependence becomes a difficult task at high strain rates. Inertia effects in the loading mechanism and the recording of the transient stress and strain in the specimen pose problems which are not easily solved. At very high strain rates wave propagation produces an uneven stress and strain distribution in the specimen which also must be taken into account if the true stress-strain relationship is to be obtained. Although a solution of these problems has been put within experimental reach through the advent of modern electronic and optical measuring and recording devices, a completely satisfactory testing method has yet to be devised.

In order to give an idea of the problem, a brief resume of some

the experimental approaches that have been made will be presented here. The list is by no means complete but will introduce the reader to the general methods of dynamic testing.

2.2.1. Hopkinson Pressure Bar

One of the first methods of measuring transient stresses was devised by B. Hopkinson[11] in 1914 and has come to be known as the Hopkinson pressure bar. A cylindrical steel bar was suspended ballistically with a small "time piece" of the same material and diameter as the bar wrung onto one end with a thin film of grease. An impact load applied to the opposite end of the bar caused a compression pulse to travel down the bar. This compression pulse would be transmitted into the time piece, but its reflection from the free face of the time piece being of opposite sign would, when it again reached the interface, cause a tensile stress across the grease joint causing the time piece to fly off. Thus the momentum captured in the time piece corresponded to a length of pulse twice the length of the time piece. The maximum pressure in that segment of the pulse could also be found from the momentum captured. Using time pieces of different lengths, the pressure-time relations of a pulse were investigated. However, a continuous pressure-time curve was not determined.

Davies[12] made a complete investigation of the Hopkinson pressure bar and also devised an electrical means of recording the pressure pulse. He used the free end of the pressure bar as one side of a parallel plate capacitor, thus converting the small displacements of the end of the bar produced by a pulse into an electrical output which could be recorded on a cathode ray oscilloscope. Continuous displacement-time and, if the

bar remained elastic, pressure-time curves could be obtained by this method. Davies also investigated the limiting values of pulse length which could be propagated down a cylindrical bar without the pulse becoming distorted.

A further adaptation of the pressure bar technique was made by Kolsky[13] in order to determine the stress-strain relations in materials at high rates of loading. A diagram of Kolsky's apparatus is shown in Figure 1. A stress pulse produced by the detonator was propagated down the length of the bar. The pulse was assumed to remain elastic and travel with the velocity $c_o = \sqrt{E/\rho}$. Then assuming the pulse was propagated without distortion and that the stress was uniform over a given cross section of the bar, conditions which would be met if the pulse duration was long compared with the time required for a pulse to travel a distance equal to the radius of the bar, the stress σ at any point would be given by

$$\sigma = \rho c_o v,$$

where v is the particle velocity. At the free end of a bar the particle velocity is twice as great as the particle velocity associated with the pulse along the length of the bar. Thus if we let u be the displacement of the end of the bar as measured by the parallel capacitor,

$$\sigma = 1/2 \rho c \frac{du}{dt} \qquad (7)$$

Kolsky inserted thin specimens between the two sections of the bar. When an incident stress pulse of magnitude σ_I struck the specimen,

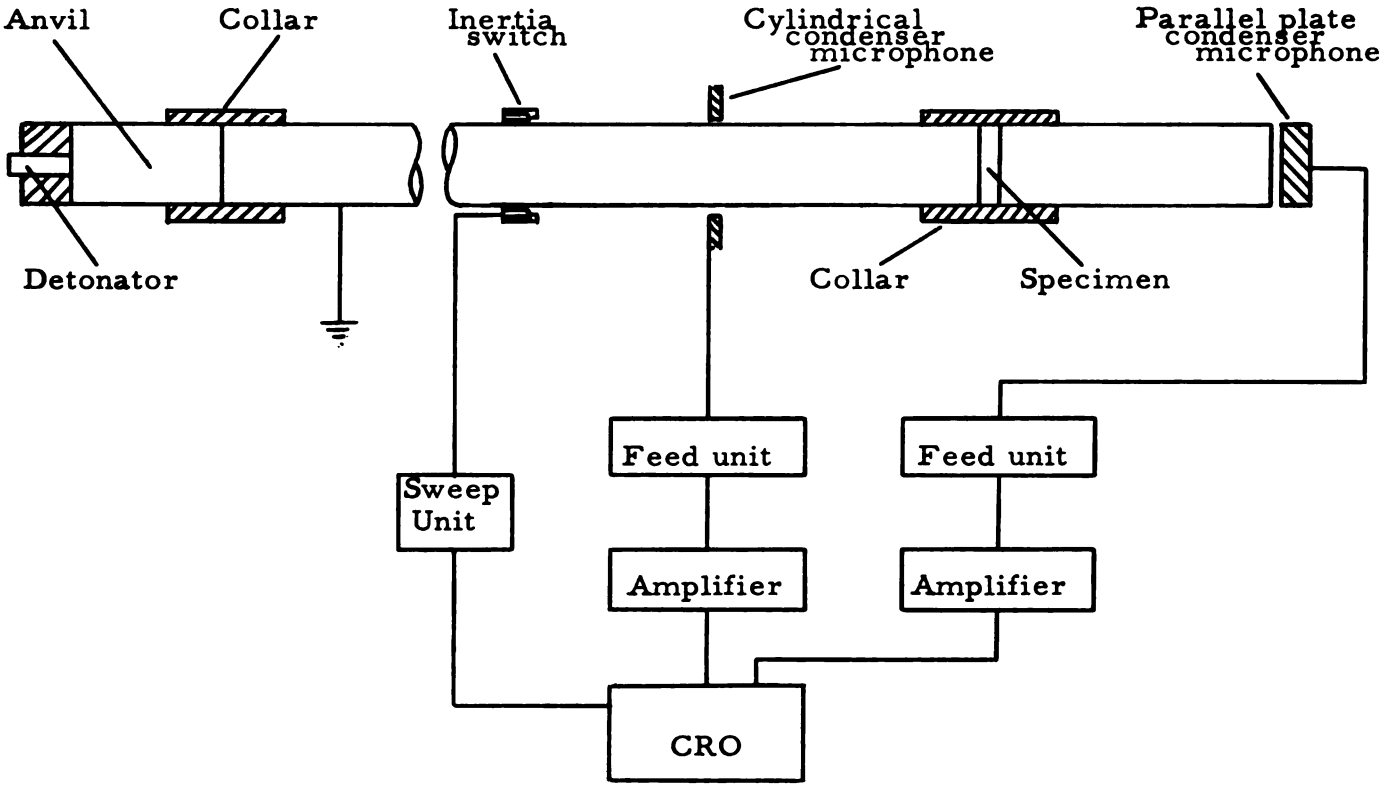

Figure 1. General arrangement of Kolsky apparatus.

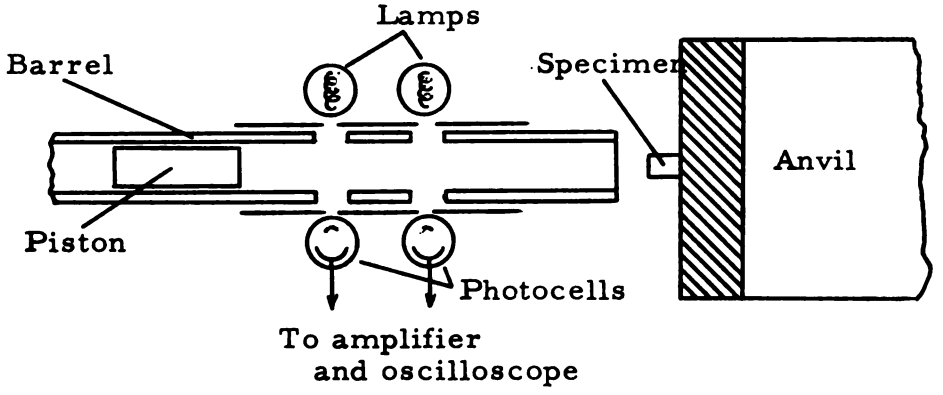

Figure 2. General arrangement of Habib apparatus.

a portion of the pulse was reflected with magnitude σ_R and part transmitted with amplitude σ_T . Assuming the stress constant across the thin specimens,

$$\sigma_I - \sigma_R = \sigma_T \tag{8}$$

Now if u_1 is the displacement of the face of the main bar in contact with the specimen at time t, then

$$u_1 = \frac{1}{\rho c} \int_o^t (\sigma_I + \sigma_R)\, dt \tag{9}$$

and if u_2 is the displacement of the face of the extension bar in contact with the specimen,

$$u_2 = \frac{1}{\rho c} \int_o^t \sigma_T\, dt\ . \tag{10}$$

If the thickness of the specimen is ℓ, the strain ϵ in the specimen is

$$\epsilon = \frac{u_1 - u_2}{\ell} \tag{11}$$

Thus using Equation (8), (9), (10), and (11),

$$\epsilon = \frac{2}{\rho c_o \ell} \int_o^t (\sigma_I - \sigma_T)\, dt \tag{12}$$

Since $\frac{2}{\rho c_o} \int_o^t \sigma_T dt = u_T$ was the displacement measured with the specimen included and $\frac{2}{\rho c_o} \int_o^t \sigma_I dt = u_I$ the displacement with the specimen absent, a strain-time curve could be calculated from

$$\epsilon = \frac{u_I - u_T}{\ell}$$

A stress-time curve was obtained by taking the gradient of the u_T curve, see Equation (7). Thus the stress-strain curve was obtained for the conditions of the experiment.

Due to the nature of the pulse produced by the detonator, the strain rate in the specimen varied throughout the test requiring a correction in the stress for lateral inertia effects. Kolsky determined this correction to be

$$\sigma - \sigma_\epsilon = 1/2\, \nu^2\, r^2\, \rho^2\, \frac{d^2\epsilon}{dt^2}\ , \qquad (13)$$

where σ_ϵ was the stress required to produce strain ϵ when no kinetic energy was imparted to the specimen and σ was the measured stress. ν and r are Poisson's ratio and the radius of the bar.

A few difficulties with this method may be noted. Since the specimens were very thin, 0.05 and 0.10 cm. thick for lead and copper, friction effects may have been important although a thin grease film was used to minimize this effect. Also the determination of the stress requires a numerical differentiation of the displacement-time curves which may introduce error. Further, two separate detonations were required to determine a single stress-strain curve. An attempt to remedy this was made by using a cylindrical capactior concentric with the main bar to measure the radial expansion due to the incident pulse, but the results from this proved to be unreliable due to distortions introduced by the bar.

2.2.2. Compression Impact

Habib[14] has indirectly arrived at stress-strain relations under impact conditions by measuring the energy absorbed by small copper cylinders when they were impacted as shown in Figure 2 by a piston fired from a compressed air gun. The energy absorbed by the specimen was determined from the difference in the impact and rebound velocity of the piston as measured by photo-electric cells. By plotting the energy absorbed E against the deformation x as determined from the initial and final dimensions of the specimen, energy-deformation curves were obtained which could be differentiated to derive the force F, since

$$E = \int_0^x F \, dx$$

or

$$F = dE/dx .$$

Each point on an energy-deformation curve was obtained from a different specimen. The energy absorbed and the deformation in the specimen could be varied by changing the mass and the velocity of the impacting piston.

Habib's results showed that the energy required to produce a given deformation always increased as the rate of straining increased. Also, the increase in dynamic stress over the corresponding static stress was a function of both the strain rate and the strain. However, as pointed out by Lee and Wolf[15], the assumption of uniform strain in the specimen when deriving stress-strain relations based on energy absorption may produce only an apparent rise in the stress-strain curve if the strain

distribution is actually non-uniform.

Turnbow and Ripperger[16] have used a setup similar to Habib's except that they measured the stress and strain in the specimen directly. This was done by placing strain gages directly on the specimen to measure strain, and by replacing the solid anvil by a Hopkinson type pressure bar instrumented with strain gages to measure the force transmitted by the specimen. The strain rates could be varied by changing the piston velocity. With sufficient mass in the piston essentially constant strain rates were achieved. With this method a continuous record of the strain could only be obtained up to the limit of the strain gages on the specimen, also proper alignment so as to insure planeness of impact becomes a difficult problem. Data from the tests performed were not sufficiently reliable to affirm the linear strain rate theory of Malvern.

Alder and Phillips[10] carried out compression tests at constant true strain rates between 1 and 100 in./in./sec. on a specially designed testing machine. In this machine the specimen was compressed to 50% reduction in height between two platens, the lower one of which was driven by a rotating cam, whose speed could be varied. The upper platen was attached to a load measuring device which consisted of two birefringent glass blocks. The change in birefringence upon application of load was recorded photographically on a rotating drum mounted on the driving shaft. The results of tests performed on aluminum, copper, and steel at various temperatures showed that in the range of strain rates used the data could best be fitted to the exponential type relationship although the logarithmic law also gave reasonable approximation.

2.2.3. Tension Impact

Perhaps the first investigators to record stress and strain directly

for dynamic loading conditions were Manjoine and Nadai[17,18,19] in 1940. Briefly their apparatus consisted of a tension specimen connected on one end to a force measuring bar and the other end to a tup which could be struck by a hammer attached to a heavy fly wheel. Displacement of the specimen and deformation in the force measuring bar were both recorded photoelectrically and fed simultaneously to the horizontal and verticle deflection plates of a cathode ray oscilloscope. In this manner the stress-strain curves were recorded directly. Constant strain rate tests, at low rates, were also carried out on another machine, so that a range of strain rates from 10^{-6} to 10^{3} in./in./sec. was covered. Tests were conducted on copper, aluminum, and mild steel at room and elevated temperatures. The results indicated that when stress was plotted against the logarithm of the rate of strain a relatively linear relationship with positive slope was obtained at the lower strain rates, indicating a logarithmic law to be valid in this region. Above about 10^{-1} in./in./sec., however, the slope of the curves gradually increased so that they bent upward and no longer remained linear. This nonlinearity was most pronounced for tests at elevated temperatures.

A serious problem encountered in the recording technique of Manjoine and Nadai was that serious oscillations occured in the records at the high strain rates due to elastic vibrations in the force measuring system. Another disadvantage to the tension test is that the specimen must of necessity be of appreciable length in order to grip it and to apply the load. Thus at the very high strain rates the distribution of strain over the length of the specimen and also the rate of straining is not uniform, due to wave propagation effects in the specimen.

This problem in dynamic tensile testing has been discussed by Clark and Duwez[20] who have also attempted to design a tensile test that would eliminate wave propagation effects[21]. Their technique consisted of subjecting thin walled cylinders to an internal pressure pulse. This pulse was obtained by impacting a piston which compressed the fluid within the cylinder. Stress-time but not strain-time was recorded for these tests, thus limiting their value.

2.2.4. Plastic Wave Propagation

Some investigators have derived dynamic stress-strain relations directly from measurements of plastic waves propagated in long rods. These techniques all utilize the von Karman-Taylor theory, particularly the relationship expressed in Equation (1).

An example of this type of technique is given by the tangent modulus method of Campbell[22]. In this method a long bar was subjected to a tensile impact by means of a freely falling weight, causing a stress pulse to travel the length of the bar. The pulse was measured directly as a function of time by two wire strain gages placed a given distance apart on the bar. As seen from the expression for wave velocity, Equation (1), the tangent modulus $\frac{d\sigma}{d\epsilon}$ is given by the relation

$$\left(\frac{d\sigma}{d\epsilon}\right)_{\epsilon=\epsilon_n} = \rho\, c_n^2$$

where c_n is the velocity of propagation at the strain level ϵ_n. Since the stress in the bar could not be measured directly, it was found by numerically integrating the curve of the tangent modulus plotted against ϵ. Thus

$$\sigma = \int_0^{\epsilon} \left(\frac{d\sigma}{d\epsilon}\right) d\epsilon \quad .$$

With these values for σ and ϵ the stress-strain curve could be plotted. The experimental results reported by Campbell were at the time only exploratory and were subject to considerable error.

Johnson, Wood, and Clark[23] have also used the von Karman-Taylor theory to determine strain in compression impact tests. However, due to the uncertainty of the basic assumption that $c = \sqrt{\frac{1}{\rho} \frac{d\sigma}{d\epsilon}}$ the results of these tests using wave propagation must be taken with some reservation. The method also does not lend itself well to obtaining data at a constant strain rate.

3. EXPERIMENTAL METHOD

3.1. Desired Objectives

From the numerous methods of attack on the problem that have been employed in the past there does not seem to be any one that is completely satisfactory. This is an indication of the difficulty of the problem. Before describing the experimental methods employed in this investigation to obtain stress-strain-strain rate relations it may be best to outline just what our objectives should be in designing an experiment that will give us reliable and useful information. We may list them as follows:

1. Perform tests such that stress-strain curves at as nearly constant strain rate as possible may be derived.

2. Obtain each complete curve from a single specimen.

3. Record instantaneous stress and strain continuously throughout the test.

4. Obtain stress and strain records well into the plastic range.

5. Obtain dynamic curves up to 1000 in./in./sec.

6. Minimize wave propagation effects that would cause non-uniformity in the distribution of stress, strain, and strain rate in the specimen.

In the present investigation an attempt was made to meet all of the above objectives.

3.2. Dynamic Tests

With the above objectives in mind an adaptation of the method of Kolsky was used in which short specimens are compressed between two segments of a Hopkinson pressure bar. A schematic of the test setup is shown in Figure 3. Two changes from Kolsky's original setup were made. First, the impact is supplied by a third striker bar fired against the incident bar. This produces a long, flat-topped pulse rather than the shorter rounded pulses produced by an explosive charge. Second, strain gages are mounted directly on the incident and transmitter pressure bars to record the strain pulse both before and after it has passed through the specimen. Thus only a single firing is required to perform each test. Also, strain-time and therefore stress-time, since the pressure bars remain elastic, are recorded rather than displacement-time as determined from the capacitor type pickup of Kolsky.

3.2.1. Impact Loader

The stress pulse was initiated in the pressure bar by impacting it with a striker accelerated by means of a commercial Hyge Shock Tester manufactured by Consolidated Electrodynamics Corporation, see Figure 4. A schematic sketch of this equipment is shown in Figure 5a.

The acceleration of the piston is achieved in this manner: A given set pressure is applied to chamber B by means of compressed

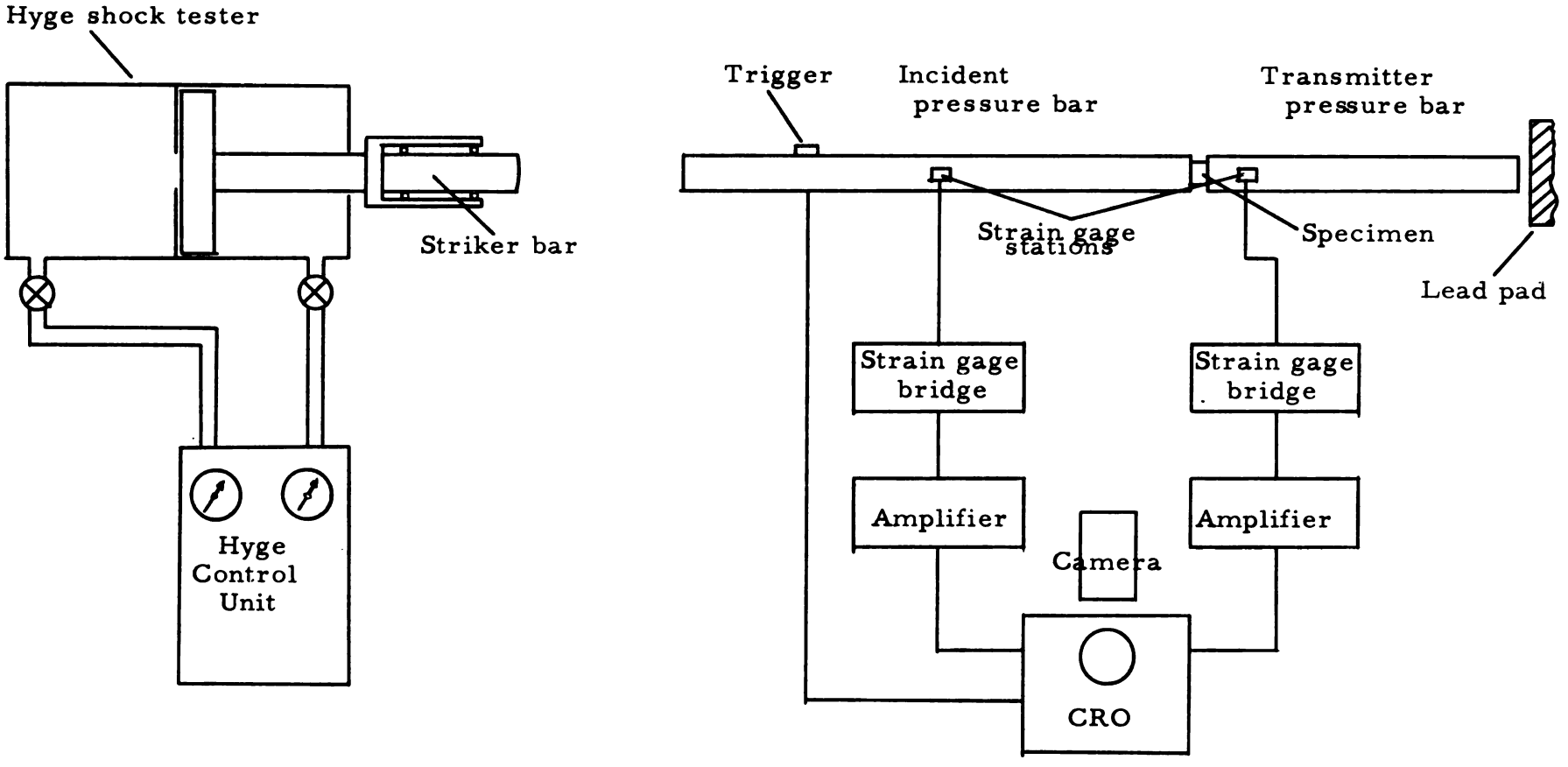

Figure 3. Experimental test setup.

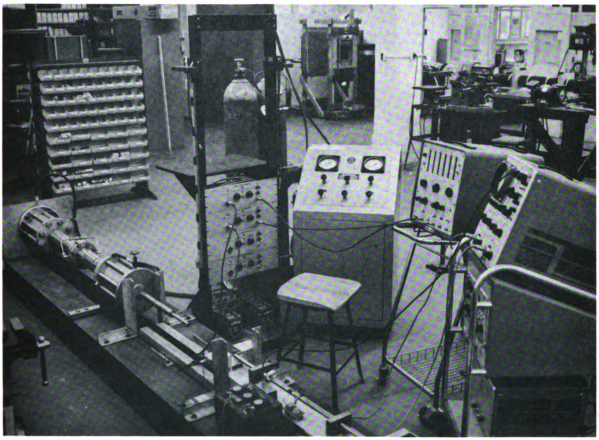

Figure 4. General View of Test Setup

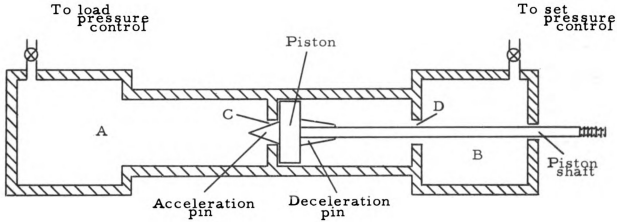

Figure 5a. Schematic of Hyge shock tester.

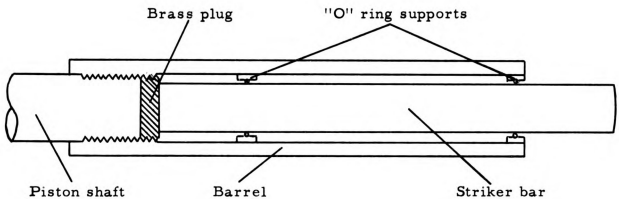

Figure 5b. Barrel with striker bar.

nitrogen. This pressure is locked in and exerts a force over the entire area of the back face of the piston. A load pressure is then applied to chamber A. This pressure acts only over the reduced piston area determined by the orifice at C. As the load pressure is increased to about four times the set pressure the forces acting on both faces of the piston become equal. An additional increase in the load pressure breaks the seal at C and the load pressure expands over the entire face of the piston resulting in a large accelerating force.

The acceleration is regulated by the acceleration pin which controls the rate at which the gas is allowed to expand over the piston. The piston is stopped by means of the deceleration pin which fits into the orifice at D. The chamber B is partially filled with oil to aid the deceleration. The entire system is controlled from a separate control panel which contains the pressure gages and control valves.

The striker bar itself rides in a "barrel" which is mounted on the end of the piston shaft as shown in Figure 5b. The barrel is a circular tube which is threaded onto the end of the piston shaft. The striker bar rides freely within the barrel supported on two rubber "0" rings. These were lightly greased so that there would be no binding of the striker bar as it moved.

The spacing between the Hyge and the incident pressure bar was such that as the piston decelerated the striker bar would just break loose from the brass plug at the base of the barrel before it struck the incident bar but would still remain supported in the "0" rings. It was essentially then a free bar upon impact. The velocity of the striker bar could be varied by regulating the set pressure in the Hyge.

The striker bar was made from 3/4 inch diameter steel drill rod, being of the same material and diameter as the pressure bars. For the majority of the tests a striker bar 16 inches long was used, although this could be varied. The length of the striker bar determines the length of the pulse produced in the pressure bar. This pulse length will be equal to the time required for an elastic wave to travel twice the length of the striker bar, due to the fact that the striker bar will rebound when the original compression pulse has been reflected from the free end and again returns to the impact face as a tensile force. In order to prevent a non-axial impact, the impact face of the striker bar was slightly rounded. This prevented impact from occurring at one edge of the striker or incident bar.

3.2.2. Pressure Bars

The arrangement and dimensions of the two pressure bars are shown in Figures 6 and 7a. Both bars were made from 3/4 inch diameter steel drill rod. The lengths of the incident bar and transmitter bar were 34 7/8 inches and 24 inches respectively. The faces in contact with the specimen were carefully turned on a lathe to a flat surface and then finished with a fine emery paper. These surfaces were made as smooth as possible in order to minimize friction effects between the bars and the specimen.

The incident and transmitter bars were each supported at two points by means of rubber "0" rings mounted in steel support blocks as shown in Figure 7b. No distortion or reflection of the pulses was found to be produced by this means of support. In order to insure uniform compression of the specimens, the bars were carefully aligned so that

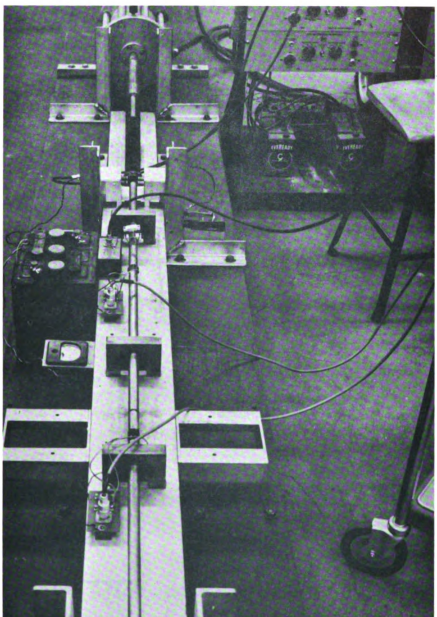

Figure 6. Close-up of Striker and Pressure Bars

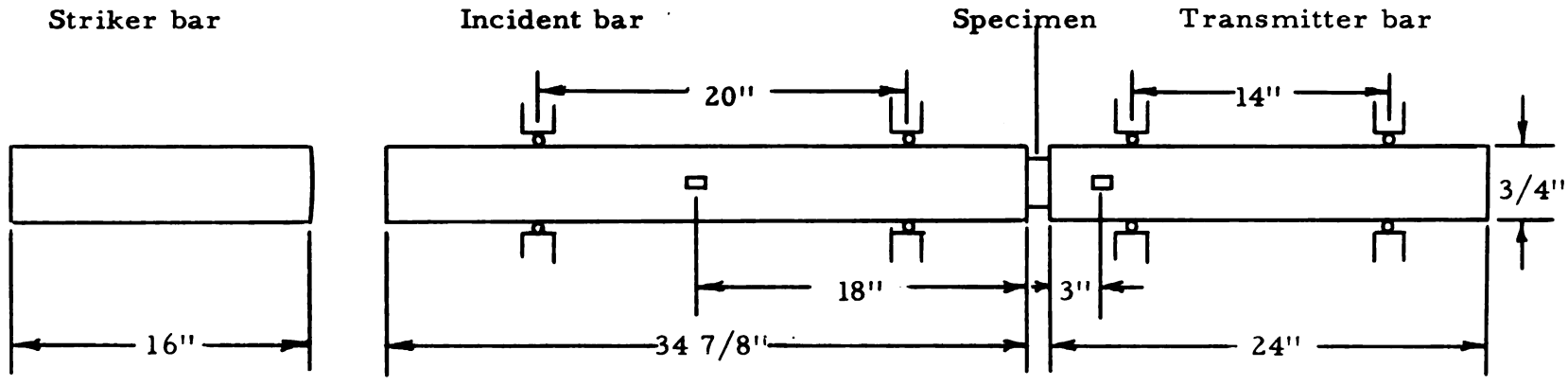

Figure 7a. Dimensions of striker and pressure bars.

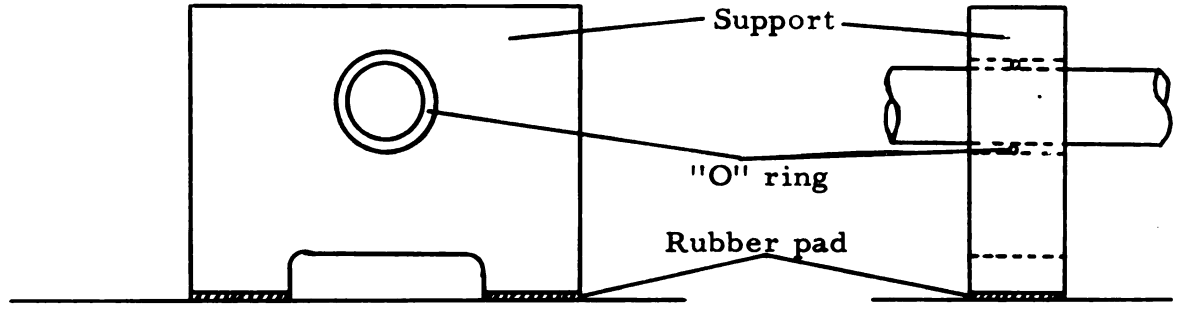

Figure 7b. Pressure bar supports.

the contact faces with the specimen would be parallel. A lead pad was placed after the transmitter bar to take up the shock from the bars after the pulse had passed through the system.

The position of the strain gages on the pressure bars was determined so that a continuous record of a single pulse could be obtained before reflections from an interface returned to the gage to mar the record. This required a length of bar equal to or greater than the length of the striker bar following each gage station. This was obtained by placing the gages 18 inches and 3 inches from the specimen on the incident and transmitter bars respectively. By placing the gages in this manner the serious oscillations produced in the records of many investigators who have used short force measuring bars was eliminated.

3.2.3. Strain gage bridges

At each gage station on the incident and transmitter bar two SR-4, type A-8, wire resistance strain gages were placed at opposite ends of a diameter of the bar. The gages were attached with Duco cement. Each gage had a resistance of 120.5 $\pm$ .3 ohms and a gage factor of 1.81 $\pm$ 2 per cent. At each station the gages were connected to the opposite arms of a Wheatstone bridge circuit, see Figure 8. The dummy gages were 120 ohm precision resistors. The bridge voltage was supplied by a 6 volt wet cell with the exact voltage recorded before each test by means of a voltmeter connected in parallel with the battery.

With the active gages placed in opposite arms of the bridge only the direct pulse was measured while any bending components of the stress were cancelled. It was assumed that for the long pulses used the amplitude would be constant through any cross section of the bar,

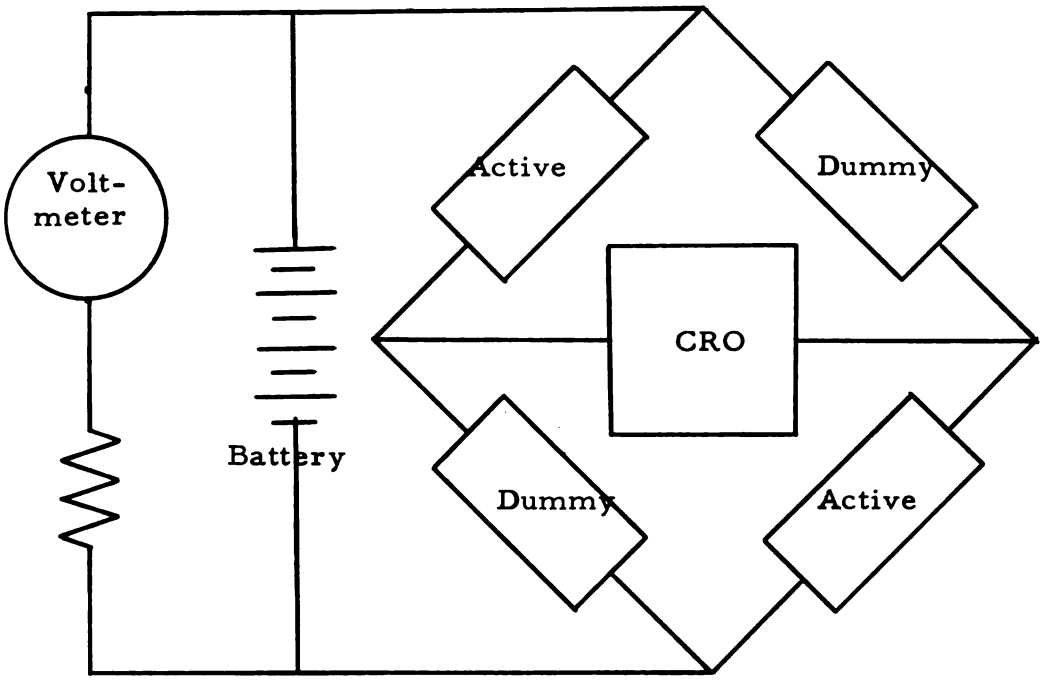

Figure 8. Strain gage bridge with two active gages.

i.e., the wave would remain plane, and that there would be no attenuation of the pulse in the elastic pressure bars.

3.2.4. Strain Recording Equipment

The output from each bridge circuit was fed into a Tektronix type 53/54E plug-in preamplifier. These are high gain, ac-coupled preamplifiers with a vertical sensitivity to 50 microvolts per centimeter and a frequency response from 0.06 cps. to 60 kc. They also permit attenuation by means of outphasing of any undesired signal through differential input connections.

The two plug-in preamplifiers were mounted in a Tektronix type 551 dual beam oscilloscope. The output from each gage station on the pressure bars was thus recorded simultaneously on seperate channels of the oscilloscope. The sweep speed of the oscilloscope could be varied continuously from 1 microsec./cm. to 5 sec./cm. By this means a complete test could be recorded on a single sweep of the dual oscilloscope beams. This sweep was triggered by means of a piezoelectric crystal pickup mounted before the first gage station on the incident bar.

A record of the oscilloscope trace was obtained by using a Dumont type 302 oscilloscope record camera with Polaroid Pola Pan 400, type 44 film. Using an open shutter at a setting of f/1.9 and an oscilloscope sweep speed of 50 microsec./cm. a clear picture of each trace was recorded.

3.2.5. Derivation of Stress and Strain in the Specimen

In order to determine the strain in the specimen as a function of time we desire to know the displacements of the faces of the incident and transmitter bars in contact with the specimen as a function of time. Let

these two displacements by u_1 and u_2 as in Figure 9. From the theory of elastic wave propagation we have

$$\epsilon = \frac{v}{c_o} = \frac{1}{c_o} \frac{du}{dt} , \tag{14}$$

where v is the particle velocity and c_o is the elastic wave velocity, a constant. On solving this equation, the displacement u is given in terms of the strain in the bar by

$$u = c_o \int_o^t \epsilon \, dt . \tag{15}$$

When a compressive pulse in the incident bar strikes the specimen, part of the pulse will be reflected from the interface as a tension pulse while part will be transmitted through the specimen to the transmitter bar as a compression pulse. The relationship between the magnitudes of these incident, reflected, and transmitted pulse will depend upon the physical properties of the specimen. The effects of the numerous internal reflections in the short specimen will be absorbed in the reflected and transmitted pulses, as the duration of these pulses is much greater than the time required for a pulse to traverse the length of the specimen. Thus, the displacement u_1 of the face of the incident bar will be the result of both the compressive strain of the incident pulse ϵ_I and the tensile strain of the reflected pulse ϵ_R. Both these strains, however, produce a displacement in the same direction, so that

$$u_1 = c_o \int_o^t (\epsilon_I + \epsilon_R) \, dt . \tag{16}$$

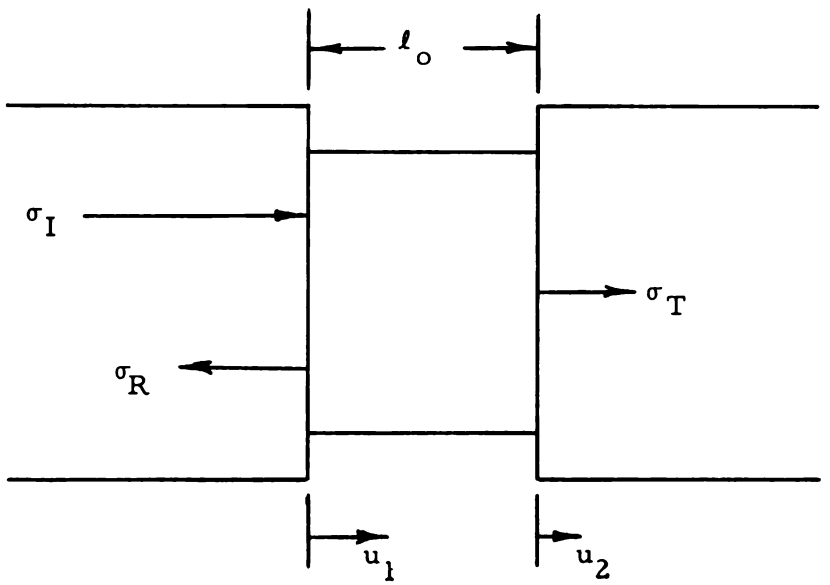

Figure 9. Schematic of specimen showing stresses and displacements.

Similarly the displacement u_2 produced by the compressive strain of the transmitted pulse ϵ_T is

$$u_2 = c_o \int_o^t \epsilon_T \, dt \tag{17}$$

In these and the following equation ϵ_I, ϵ_R, and ϵ_T denote absolute magnitudes of these quantities.

If we assume that the stress is constant across the specimen, from continuity we have

$$\sigma_I - \sigma_R = \sigma_T \tag{18}$$

Dividing this equation by **E**, the modulus of elasticity of the bars, we get

$$\epsilon_R = \epsilon_I - \epsilon_T \ .$$

Substituting this in Equation (16),

$$u_1 = c_o \int_o^t (2\,\epsilon_I - \epsilon_T) \, dt \ . \tag{19}$$

Taking ℓ_o as the initial length of the specimen, the strain in the specimen ϵ_s is

$$\epsilon_s = \frac{u_1 - u_2}{\ell_o}$$

or by substituting from Equations (17) and (19),

$$\epsilon_s = \frac{2c_o}{\ell_o} \int_o^t (\epsilon_I - \epsilon_T) \, dt \tag{20}$$

where ϵ_I and ϵ_T are the strains measured as functions of time by the strain gages on the incident and transmitter bars. Equation (20) is equivalent to Equation (12) as derived by Kolsky if the relationship $E = \rho c_o^2$ is used.

The stress in the specimen is obtained directly from the record of the transmitted pulse, since

$$\sigma = E \epsilon_T \quad . \tag{21}$$

It may be noted that by direct measurement of the strains a differentiation of the displacement-time curve to determine stress is eliminated. However, this is replaced by the necessity of a numerical integration in calculating strain in the specimen.

3.3. Low strain Rate Tests

In order to obtain data over a wide range of strain rates and to correlate the dynamic with "static" behavior, compression tests were run at three different speeds on a standard testing machine.

3.3.1. Testing Machine

All tests at low strain rates were performed on a model FGT Baldwin-Emery SR-4 Universal Testing Machine. The testing speed range of this machine controlled by a variable speed motor is 0.025 to 9.00 inches per minute. A general view of the machine is shown in Figure 10.

The specimens were compressed between two 3/4 inch diameter steel columns. The faces of these two columns were ground flat and finished with fine emery paper. The specimens were the same size as those used in the dynamic tests so that the results could be compared.

3.3.2. Stress and Strain Recording

At strain rates of 1.67×10^{-3} and 3.33×10^{-4} in./in./sec. con-

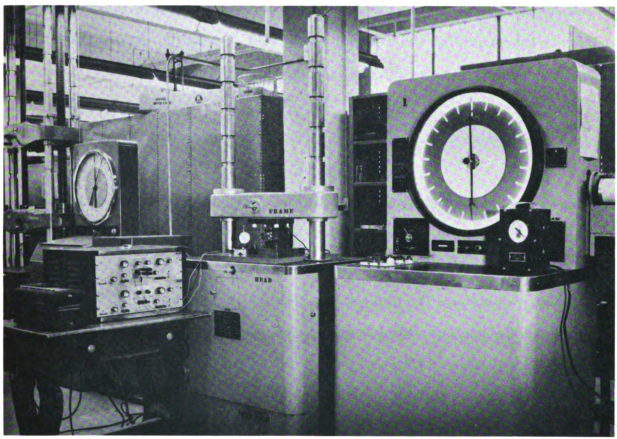

Figure 10. Baldwin-Emery Testing Machine with Stress and Strain Recording Equipment

tinuous load-deflection curves were obtained by using Baldwin Automatic Stress-Strain Recorder, Model MA-1B. On this recorder the strain axis is driven by a microformer type extensometer. A Baldwin Model TS-M extensometer was used. The extension arms of the microformer, see Figure 11, rested on two clips attached to the upper and lower load columns. Displacement was measured between two points each 1/8 inch from the faces of the load columns. The strain in the steel columns between these two points was negligable in comparison with the strain in the specimens and was neglected.

The load axis on the automatic recorder is driven by the output from the load cells in the testing machine itself.

In these tests a constant rate of straining was maintained by the use of a Baldwin Strain Rate Pacer. In this instrument a needle is driven by the output from the microformer at a rate corresponding to the strain in the specimen. This needle is paced to the speed of a coaxially mounted background wheel driven at a constant speed by means of a synchronous motor. The speed of the background wheel could be varied by changing gear ratios.

For strain rates on the order of 10^{-1} in./in./sec. the frequency response of the Baldwin automatic recorder was insufficient so that a two channel Brush pen oscillograph recorder was used instead. Stress-time and strain-time were recorded simultaneously on the two channels. In this setup the microformer extensometer was connected to a low voltage differential transformer balance unit in a Brush universal amplifier, Model RD 5612-00. The output from this amplifier was connected to one channel of the oscillograph.

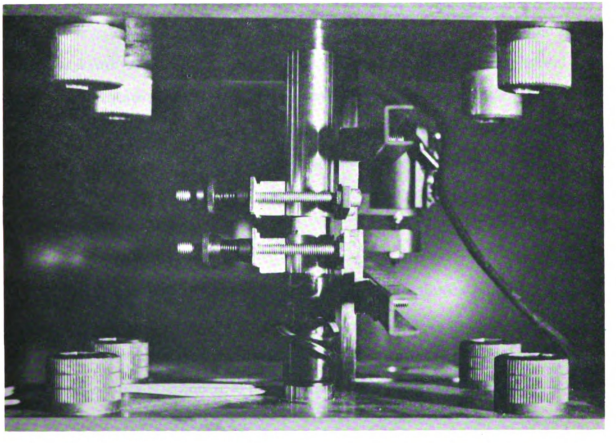

Figure 11. Close-up of Testing Jig with Microformer

To measure load two semiconductor strain gages were mounted on opposite sides of the bottom load column. These gages were Kulite, Type DA-101 with a gage factor of 118 $\pm$ 5 and a resistance of 65 $\pm$ 2 ohms. Gages with this high gage factor were necessary because of the small strains produced in the steel column by the loads required to compress the specimens. As it was necessary to mount these gages on a flat surface, shallow flats were ground on the round column. The two gages were connected to opposite arms of a bridge balancing unit of a second Brush amplifier. Precision resistors were used in the other arms of the bridge. The output from this amplifier was fed to the second channel on the oscillograph.

The time axis of the oscillograph record was determined by the chart feed speed. For the tests performed this speed was 125 cm. per second.

3.4. Specimens

In the present investigation three different metals were tested; lead, aluminum, and copper. These were selected as they were common metals and are sufficiently softer than the steel pressure bars, a requirement of this method if appreciable strains are to be produced in the specimen. The crystal structure of all three metals is face centered cubic.

The lead specimens were made from commercially pure lead sheet stock. This lead was melted down and molded into blanks 1/2 inch in diameter and 1/2 inch long. These blanks were then turned down and faced on a high speed collet lathe to the proper thickness. The machined specimens were annealed at 200^{o}F for two hours.

The aluminum was from No. 1100 (2S), 1/2 inch diameter aluminum

rod. The specimens were cut from the rod and faced on the collet lathe. Annealing was at 600°F for two hours.

Copper specimens were similarly machined from 1/2 inch diameter commercially pure soft copper bar stock and were annealed at 650°F for two hours.

The thickness of all the specimens used in the dynamic and low strain rate tests was 0.250 inches which was determined so that consistent results could be obtained as will be described later. Using 1/2 inch diameter specimens with the 3/4 inch diameter pressure bars assured that uniform displacement of the faces of the specimen would be maintained throughout the test. Originally 1/2 inch diameter specimens were used with 1/2 inch diameter pressure bars, but as the strain increased, the material squeezed out from between the bars formed a ring which it was felt would affect further compression of the specimen.

4. EXPERIMENTAL PROCEDURE

4.1. Dynamic Tests

4.1.1. Determination of Elastic Wave Velocity

In order to calculate strain in the specimens the elastic wave velocity c_o in the steel pressure bars must be determined. This was done by measuring the time required for a single pulse to travel twice the length of the incident bar. The output from the strain gage station on the incident bar was fed through a Tektronix Type 122 Low Level Preamplifier to a Hewlett Packard Electronic Counter. The preamplifier was necessary in order to supply enough voltage to trigger the counter. With the incident bar supported as a free-free bar a strain pulse with a short rise time (on the order of 15 microseconds) was produced upon

impact from the striker bar. A time count on the counter was started by the initial strain pulse traveling down the bar and was stopped by the pulse when it again reached the gage station after having been reflected from the far end of the bar, back to the impact surface, and again to the gage station, a distance of twice the length of the bar. The sharp rise time of the pulse provided an accurate trigger for the counter so that consistant results within one microsecond were obtained. By this method c_o was determined to be 198,000 in./sec.

4.1.2. Dynamic Calibration of Strain Gages

For the elastic impact between the striker and pressure bar we may derive an expression between the impact velocity and the maximum strain in the compression pulse. Consider the pressure bar to be stationary and to be struck by the striker bar traveling at velocity v_s. Both bars have the same cross sectional area A, density ρ, and elastic wave velocity c_o. At the moment of impact a wave of compression travels away from the interface into both bars at the velocity c_o. Behind the wave front there will be a region of constant strain which will be maintained until unloading occurs due to reflection from the opposite end of the shorter bar.

At time t the compression will have travelled a distance $c_o t$ into each bar as in Figure 12. If F is the contact force between the two bars and we apply the impulse momentum equation to each bar we obtain for the pressure bar

$$Ft = (\rho A c_o t) v_p ,$$

where v_p is the particle velocity acquired by the mass $(\rho A c_o t)$ due to

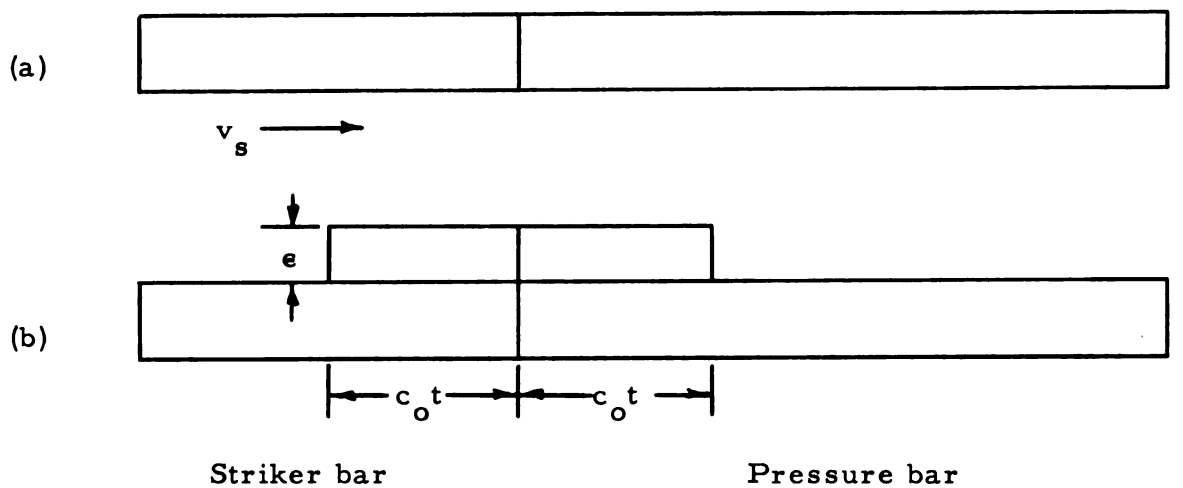

Figure 12. Striker and pressure bar (a) at moment of impact, and (b) after time t.

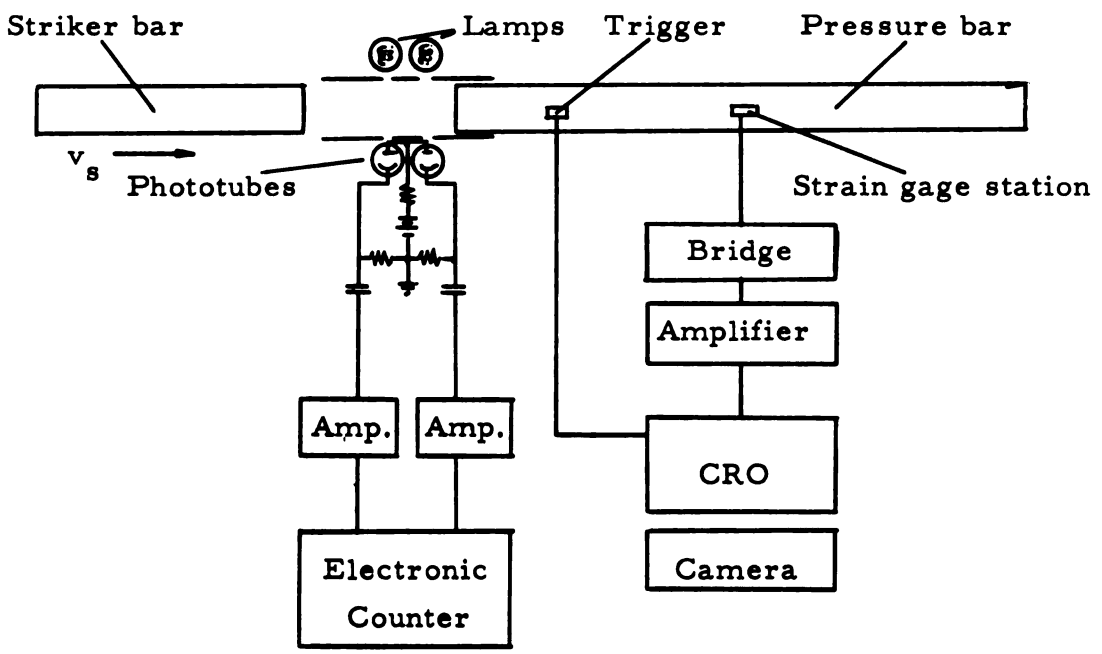

Figure 13. Setup for calibration of strain gages.

the impulse Ft. Similarly during the same time the striker bar receives impulse

$$- Ft = (\rho A c_o t)(v_p - v_s) .$$

By equating the impulses we get

$$v_p = \frac{v_s}{2} \qquad (22)$$

For a region of uniform strain $c_o t$ in the pressure bar, the displacement will be given by $v_p t$. Therefore the strain is

$$\epsilon = \frac{v_p t}{c_o t} = \frac{v_p}{c_o} . \qquad (23)$$

To dynamically calibrate the strain gages in this experiment, a series of tests were run at varying impact velocities. The output from a strain gage bridge as recorded on the oscilloscope was then calibrated against the maximum strain as computed from Equation (23).

In order to measure the impact velocity of the striker bar a photocell setup was employed as shown in Figure 13. Two IP42 photo tubes with separate light sources were placed behind two narrow slits one inch apart immediately before the impact face of the pressure bar. The output from the first tube after being amplified was connected to the start input on an electronic counter. The amplified output from the second tube was connected to the stop input of the counter. As the striker bar successively cut the two light beams a time count by the counter was started and stopped, thus recording the time interval for the striker to travel one inch. As the striker bar at this point was

riding free in the barrel, any acceleration or deceleration in this short distance was neglected. The impact velocity v_s was then taken as one inch divided by the time recorded on the counter. By varying the set pressure on the Hyge, striker velocities between 17 and 37 ft./sec. were achieved.

Strains calculated from the equation

$$\epsilon = \frac{v_s}{2c_o} \tag{23a}$$

were then compared with results using the strain gage bridge equation

$$\epsilon = \frac{2}{V_o F} \Delta v , \tag{24}$$

where V_o is the applied bridge voltage, F is the gage factor for a single gage, and Δv is the change in voltage produced by the strain ϵ as determined from photographic records of the oscilloscope trace. It was found that if the manufacturers gage factor of 1.81 was used the difference between Equations (23a) and (24) was less than 2 per cent over the range of impact velocities used, see Figure 14. Thus Equation (24) was used to calculate strain in the ensuing tests.

4.1.3. Check on the Uniformity of Stress in the Specimen

In order to check on the assumption of Equation (18) that the stress across the specimen is uniform, it was necessary to obtain a clear record of all three pulses, incident, reflected, and transmitted. The incident and reflected pulses could both be recorded on the single gage station on the incident bar if a striker bar somewhat shorter than the distance between the gage station and the specimen was used. The incident pulse would then have completely passed the gage station before its reflection

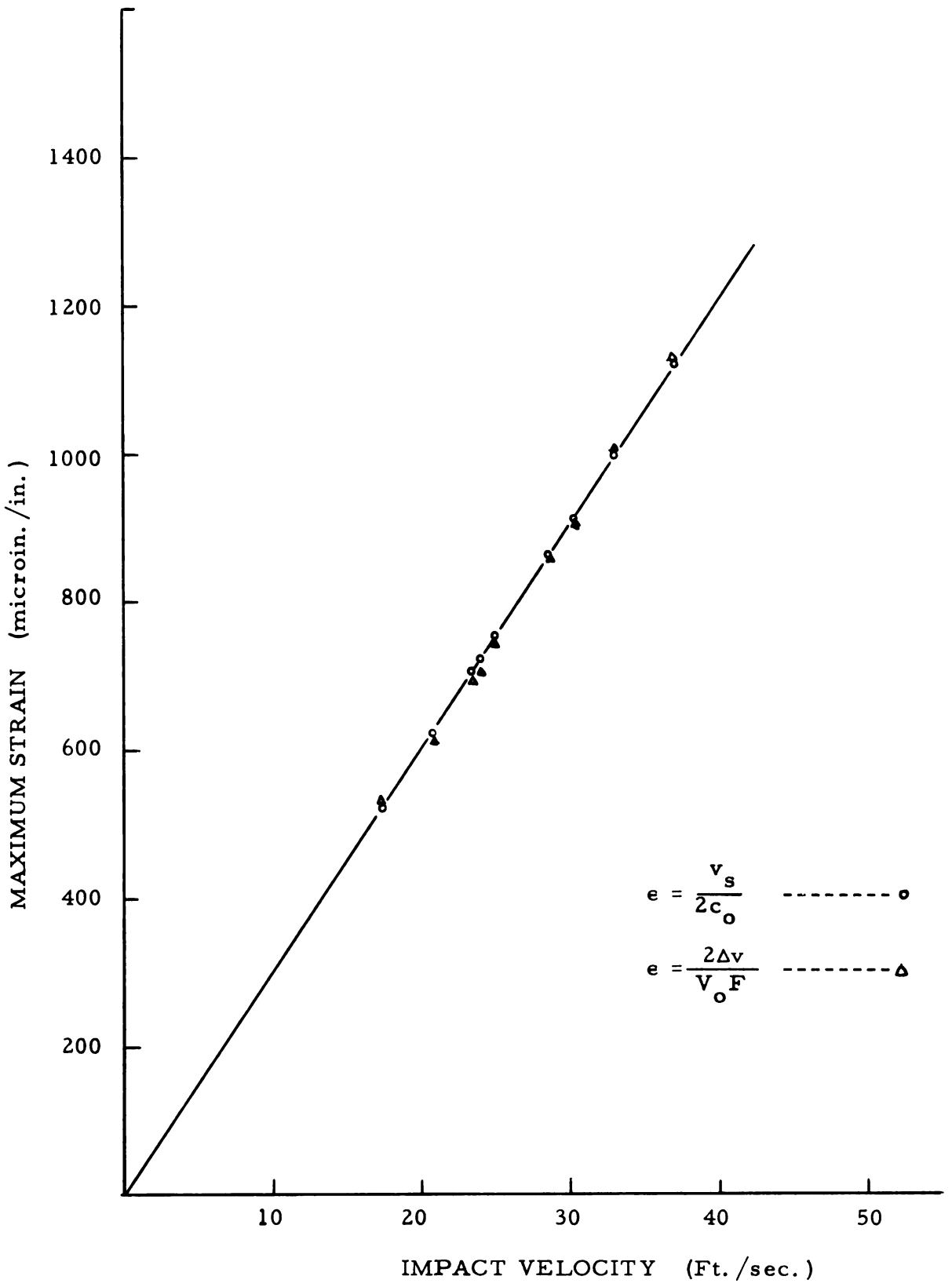

Figure 14. Comparison of strain determined from impact velocity and the strain gage bridge equation.

returned from the interface with the specimen.

In tests on lead specimens of thicknesses up to 0.250 inches it was found that during the flat portion of the incident pulse the assumption of Equation (18) was fairly good, there being only a slight decrease in stress, generally less than 3 per cent. During the sharp rise time, however, there tended to be considerable error. This was probably due to a greater attenuation of the higher frequency components of the pulse, both in the specimen and in the elastic pressure bars. For this reason and due to the lack of accuracy in measurement during the sharply rising portion of the pulse, values obtained at low strains are somewhat in doubt. Thus with the type of pulse used in this investigation the elastic behavior of the specimens cannot be accurately determined. However, above about 2 per cent strain there will be little error in using Equation (20) to determine strain.

4.1.4. Evaluation of the Effect of Friction

When using very short compression specimens the effect of friction is always an unknown quantity. In order to determine whether there was a minimum thickness that could be used that would be independent of friction or size effects a series of tests were run on lead specimens ranging in thickness from 0.108 to 0.300 inches. Any effect of the thickness on the dynamic stress-strain curves could then be noted.

Specimens of five different thicknesses, 0.108, 0.200, 0.250, 0.275, and 0.300 inches were tested. The results of one series of tests at a single impact velocity are given in Figure 15. When testing the specimens a thin coat of lubricant was applied to each face. The best lubricant that was found for this purpose was molybdenum disulfide,

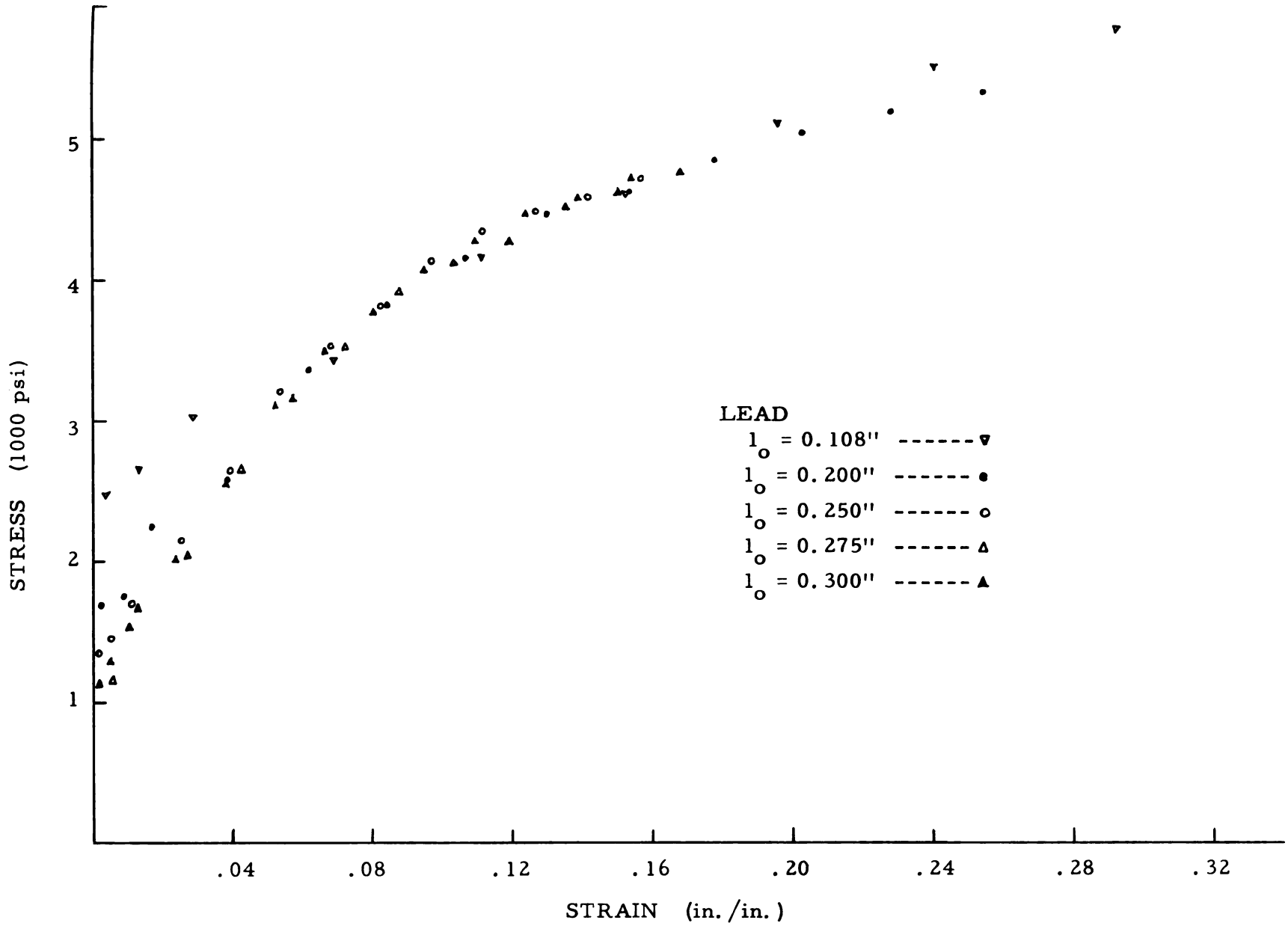

Figure 15. Stress-strain curves for lead specimens of varying thickness.

commercially called Molykote. In static compression tests on very thin specimens this lubricant was found to be much superior to other types that were tried.

From Figure 15 it is seen that at the two lower thicknesses a considerable increase in the stress at the lower strains occurs, although above about 5 per cent strain these curves coincide well with those of the thicker specimens. Since this series of curves was obtained with the same impact velocity and therefore incident loading pulse, there is some variation in the strain rate, the thinner specimens having a higher strain rate due to the fact that they have a shorter gage length. In order to ascertain that the high initial increase in stress in the thin specimens may not have been due to a strain rate effect only, the same series of tests was run at different impact velocities. These tests showed that the large initial jump in stress was characteristic of the thin specimens and not of the strain rate. If very thin lead specimens, say 0.030 inches, were used, the initial jump in stress, as shown by the transmitted pulse, appeared as a large oscillation on the stress-time record. On the records for the thicker specimens this oscillation was still noticeable, see Figure 16, but is considerably damped out. This phenomena was much more pronounced in lead than in the other metals tested.

It seems doubtful that the variation in stress at low strains was due to friction, a factor which should become more important at the higher strains. Another measure of the friction effect is obtained, however, by the amount of barreling in the compressed specimens. Only slight barreling was noticed at the higher strains indicating that friction effects were small.

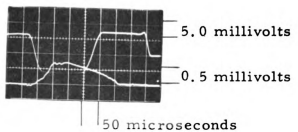

(a) Lead

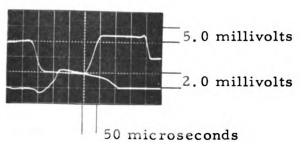

(b) Aluminum

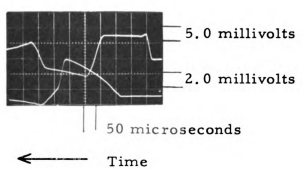

(c) Copper

Figure 16. Typical oscilloscope records for 1/4 inch long lead, aluminum, and copper specimens. Incident and transmitted pulses are shown on the upper and lower channels respectively.

Above 0.250 inches the variation of the thickness in the lead specimens does not seem to affect the stress-strain curves. For this reason a specimen thickness of 0.250 inches was used in all of the dynamic and low strain rate tests.

4.1.5. Testing Procedure

In performing the dynamic tests the following procedure was followed:

1. The oscilloscope with plug-in preamplifiers was calibrated for amplitude by means of the square-wave calibrator output incorporated in the oscilloscope. The sweep rate of the oscilloscope had been calibrated with one microsecond timing markers previous to these tests by a factory representative. These calibrations were performed against a graticule-scale placed over the face of the cathode ray tube.

2. A specimen with a thin coat of Molykote on each surface was placed between the two faces of the incident and transmitter pressure bars. The specimen was centered by means of a spacing jig. With the pressure bars firmly pressed against the specimen the surface tension of the Molykote was sufficient to hold it in place.

3. The oscilloscope was set on single sweep lockout so that the entire test was recorded on one sweep. This required a sweep speed of 50 microsec./cm. The sweep was set to trigger on the output from the crystal mounted about 6 inches before the first gage station.

4. With a fixed set pressure locked in the Hyge the load pressure was gradually increased.

5. Just before the Hyge fired the shutter on the oscilloscope camera was opened and was held open until after the firing and the test was completed.

6. Upon releasing the load pressure in the Hyge, the piston was again seated and ready for another test.

In general it was necessary to check the set pressure on the Hyge by means of the pressure gages on the control panel before each test in order to assure that a given impact velocity would be reproduceable. Even then variations were apt to occur.

For lead and aluminum four specimens each were run at four different set pressures; 15, 30, 45, and 60 pounds. For copper two specimens each were run at 15 and 60 pounds set pressure.

4.1.6. Reduction of Data

Measurements from the photographic records of the oscilloscope traces were made using a Pye two-dimensional measuring microscope accurate to 0.01 mm. Amplitudes of the incident and transmitted pulses were measured vs. time. The time axis for the two pulses was made to coincide by using the fixed distance between the two gage stations and the wave velocity in the bars.

Nominal strain was calculated from Equation (20) by plotting $(\epsilon_I - \epsilon_T)$ vs. t and then numerically integrating this curve. True or logarithmic strain ϵ_n was then determined from

$$\epsilon_n = \ln (1 + \epsilon)$$

Taking into account the change in diameter between the specimen and the pressure bar and assuming there is no volume change in the specimen during compression, the true stress σ_n in the specimen is

$$\sigma_n = \frac{D^2}{d^2} E \epsilon_T (1 + \epsilon)$$

where D and d are the initial diameters of the pressure bars and the specimen respectively, E is the modulus of elasticity of the pressure bars taken as 30×10^6 psi., and ϵ is the nominal strain in the specimen. All stress-strain curves plotted are for true stress and true strain.

4.2. Low Strain Rate Tests

Before performing the compression tests on the Baldwin testing machine the dial load indicator was calibrated with a Morehouse Proving Ring and found to be accurate within one per cent. The load scales on both the automatic stress-strain recorder and the Brush oscillograph were then calibrated from the dial indicator. The deflection scales on both these recorders were calibrated against the displacement between the two faces of the load columns as measured with an Ames dial gage accurate to 0.0001 inch.

Specimens used were the same as those used in the dynamic tests. Molykote was used to lubricate the surfaces in each test.

At the two lower strain rates of 1.67×10^{-3} and 3.33×10^{-4} in./in./sec. the strain rate was controlled throughout the test by means of the strain rate pacer and the manual load controls on the testing machine. Although by this method a constant nominal rather than true strainrate was obtained, in plotting the results this difference was neglected as it was not found to be significant up to the maximum strains attained. With a specimen centered between the load columns, the oscillograph was turned on and the testing machine thrown in gear. The test was completed in about one second. A small gap was left between the specimen and the upper load column before starting the test so that the machine could come up to full speed before starting to compress the specimen. The load and deflection channels on the oscillograph were calibrated just prior to each test.

Two specimens of each metal were run at each strain rate. Load and deflection data from all the records were converted into true stress-strain curves.

5. RESULTS

5.1. Oscilloscope Records

Typical records of oscilloscope traces for lead, aluminum, and copper are given in Figure 16. In these records the time scale reads from right to left. The upper trace on each record is the output from the gage station on the incident bar, while the lower trace is from the gage station on the transmitter bar. Along with the incident pulse, the main portion of the reflected pulse may also be seen on the upper trace, although its leading edge runs into the tail of the incident pulse. The shape of the reflected pulse corresponds to $\epsilon_I - \epsilon_T$, the function which is integrated to give the strain in the specimen, see Equation (20).

As was noted previously for the case of lead, a small initial rise occurs at the beginning of the transmitted pulse for each metal. This initial rise occurs during the period when there is a rapid acceleration in the strain due to the sharp rise time on the loading pulse. The initial apparent increase in stress thus may be attributed to inertia effects in the specimen, as seen from Equation (13).

In lead the initial rise is followed by a series of small oscillations, the period of which is from 8 to 10 microseconds. This corresponds to the period of an elastic wave in the lead traveling twice the length of the specimen. Thus, these oscillations would appear to be associated with internal reflections in the specimen. As they are very small in amplitude and rapidly damped out, it is difficult to make any

definite conclusions. It is also possible that they arise due to the change in diameter between the specimen and the transmitter bar, although this is doubtful as they were also present when 1/2 inch diameter specimens were used with 1/2 inch diameter pressure bars.

From the oscilloscope records it may also be noted that the length of the transmitted pulses are greater than the incident pulses, especially in the softer metals. This increase in length may be attributed to internal damping in the specimen. There is actually a continued increase in stress in the transmitted pulse for a short interval after the stress in the incident pulse has begun to decrease. This is somewhat obscured in the records shown because the return of the reflected pulse cuts off the tail of the incident pulse. With the 16 inch striker bar the stress should start to decrease approximately 160 microseconds after the initiation of the pulse. The initial decrease in stress in the transmitted pulses, however, occurs somewhat after this 160 microseconds depending upon the material.

5.2. Deformation in the Specimens

A photograph of several deformed dynamic specimens is shown in Figure 17. The appearance of the dynamic and the static specimens was similar after testing. Up to the maximum strains attained in this investigation there was little evidence of barreling.

Two different types of lead specimens are shown because of their marked difference in appearance. One type (specimens Pb250-15, 17, and 28) shows definite lines of flow radiating from the center of the specimen and a very coarse radial surface indicating that plastic flow did not take place uniformly throughout the specimen. The other lead specimens (Pb250-10, 20, and 27) have a more uniform appearance similar to the

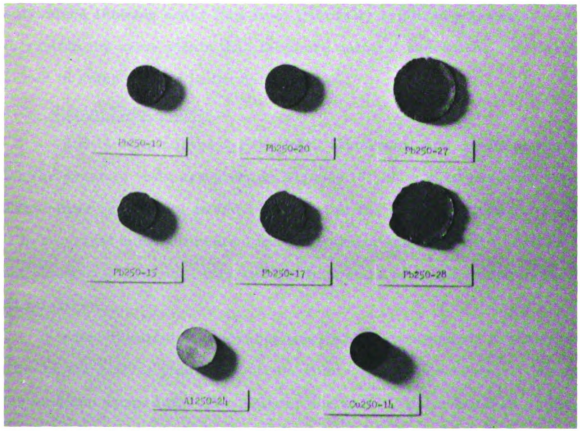

Figure 17. Deformation in Dynamic Test Specimens

aluminum (Al250-24) and the copper (Cu250-14). This difference in the two types of lead specimens did not appear to be a function of the strain rate or the maximum strain, but rather due to some variation or non-uniformity in structure between the different specimens. As each lead specimen was molded individually variations were liable to occur. The specimens showing heavy flow lines generally required a lower stress to sustain the same strain than the more uniform specimens. This resulted in some scatter in the data for lead.

5.3. Strain-Time Curves

Strain-time curves for the lead, aluminum, and copper specimens for the dynamic tests are given in Figures 18, 19, and 20 respectively. Each curve represents an individual test at the indicated Hyge set pressure. It is seen that accurate control over the strain rate with set pressure was not obtained. However, this was not important as only a range in rates was desired.

After the first 20 microseconds, which corresponds to the rise time on the loading pulse, the strain-time curves become nearly linear for lead and aluminum. For copper, due to its greater hardness, there is some deviation from linearity, but for the purposes of this experiment an average strain rate was taken. It was felt that the deviations were not of sufficient magnitude to affect the conclusions.

The range of strain rates attainable by this pulse type loading is unfortunately limited. Significant extensions beyond the range of 600 to 3000 in./in./sec. obtained in this investigation are not feasable. In order to lower the strain rate to 100 in./in./sec., the duration of the test and therefore the incident pulse must be on the order of 1 millisecond

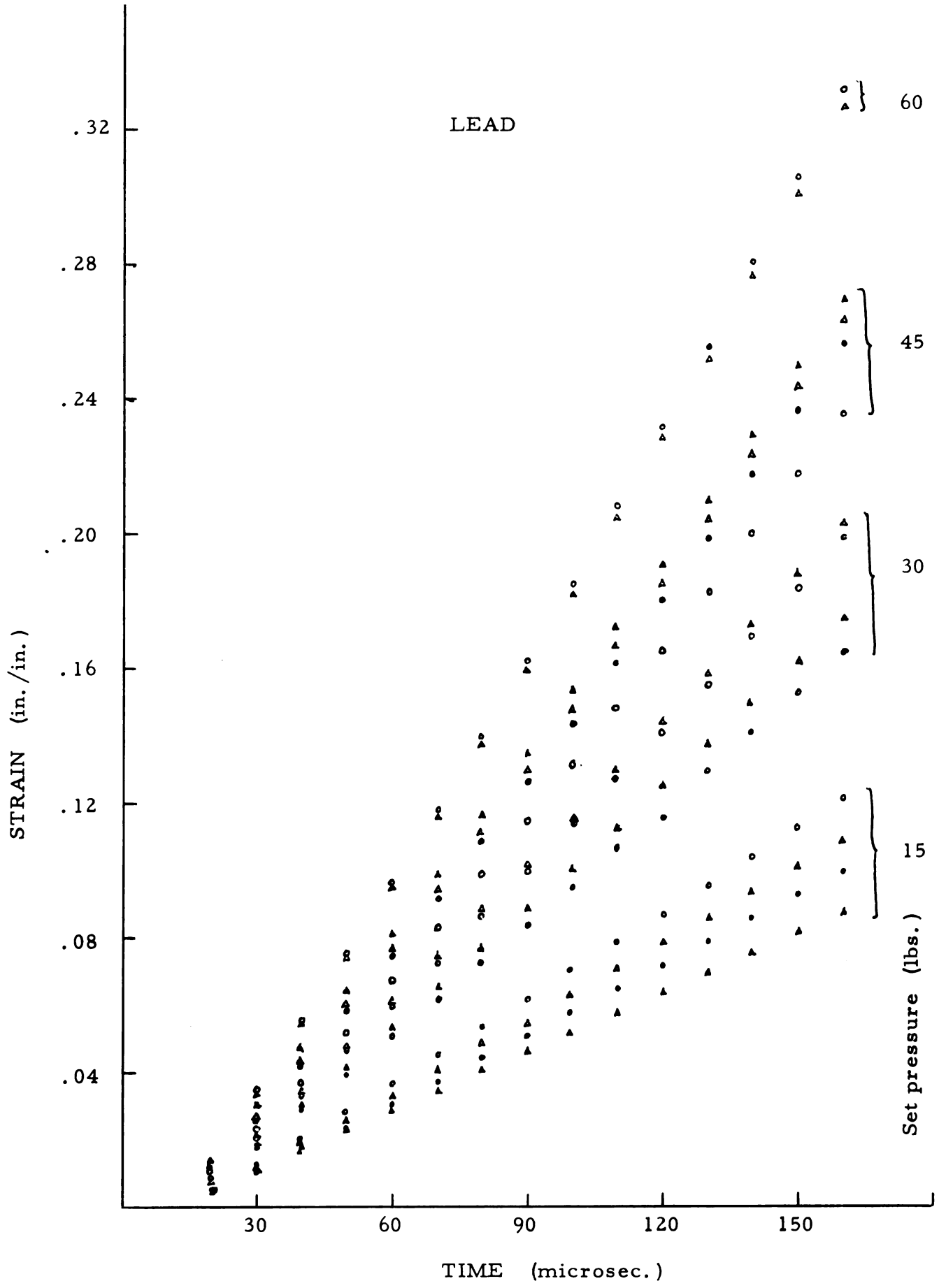

Figure 18. Strain-time curves for lead.

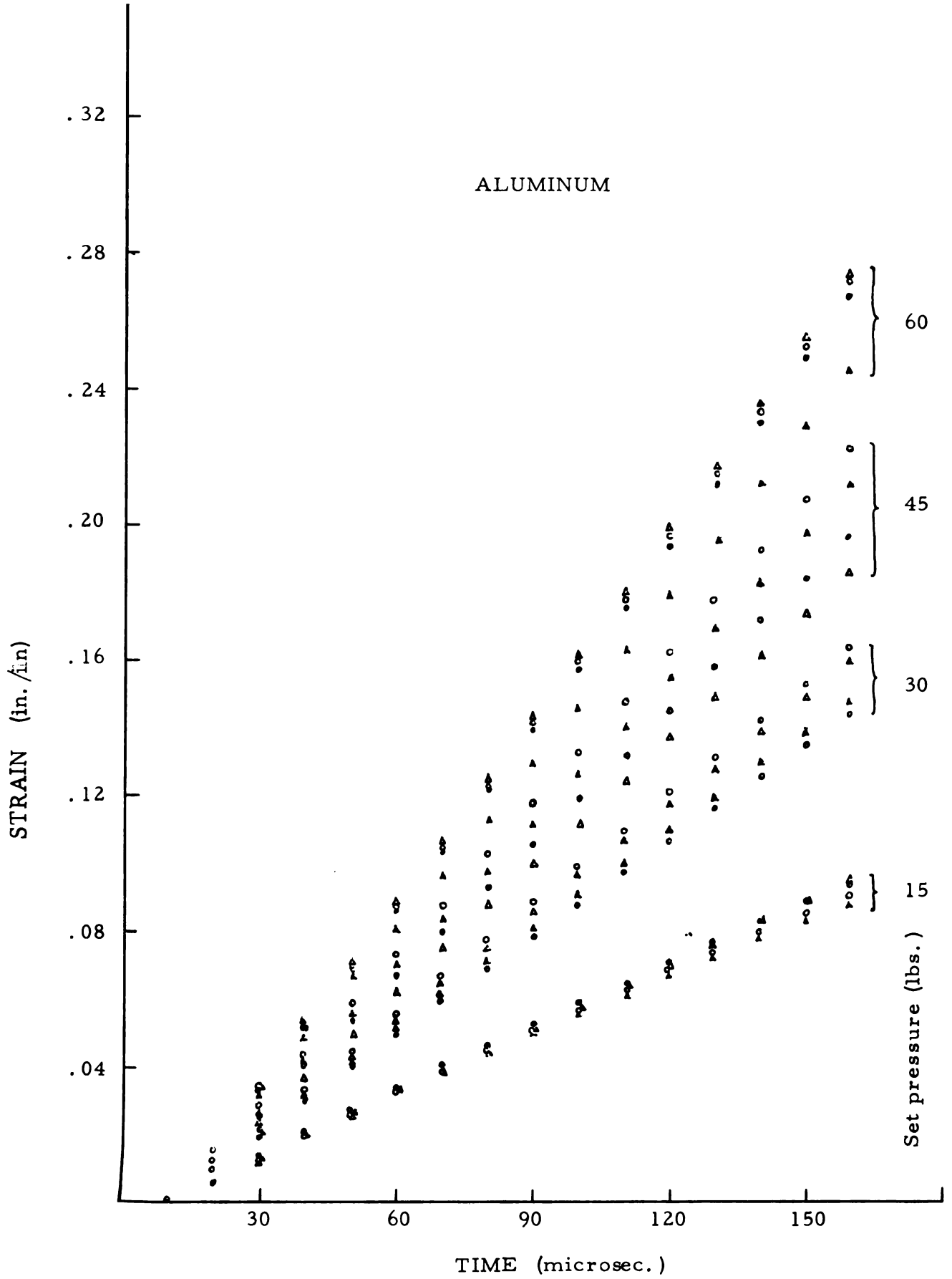

Figure 19. Strain-time curves for aluminum.

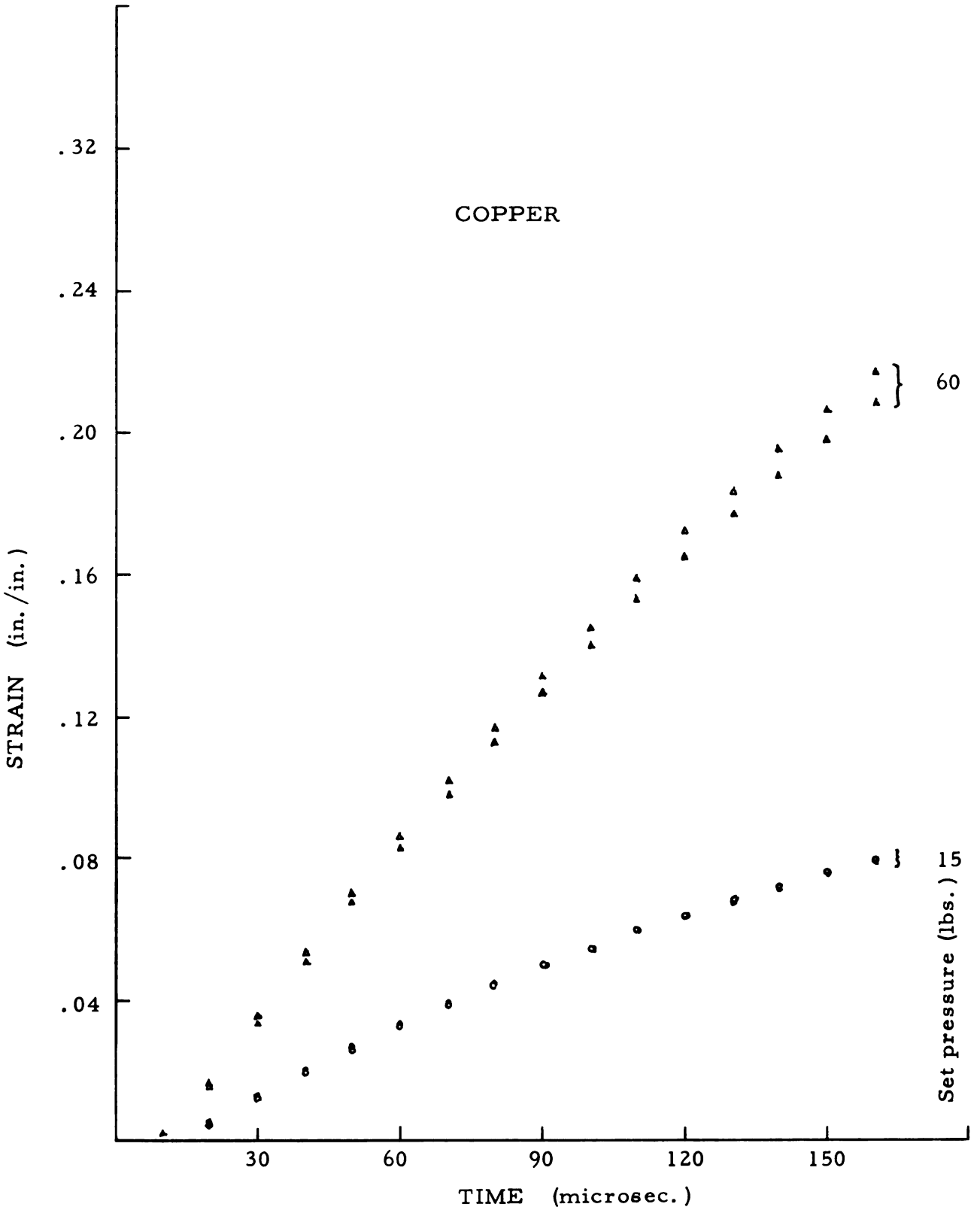

Figure 20. Strain-time curves for copper.

if a maximum strain of 10% is to be acheived. This would require a striker bar of 100 inches in length with a corresponding increase in length of the pressure bars, making the apparatus unwieldy. The amplitude of the incident pulse must also be reduced to a level at which the strains would become more difficult to measure. On the other hand, in order to increase the strain rate the amplitude of the incident pulse must be increased and the duration of the test shortened. The amplitude of the incident pulse, however, is limited by the condition that the pressure bars must remain elastic. Also by having large strains occuring in a short time, most of the strain would be achieved during the rise time of the loading pulse when the strain rate is not constant. The narrow range of uniform strain rates attainable by this method is thus a limitation on the usefulness of the method.

5.4. Stress-Strain Curves

The dynamic stress-strain curves for lead, aluminum, and copper are given in Figures 21 - 29. The curves are grouped according to the Hyge set pressure used for each test and therefore according to strain rate, see Figures 18 - 20.

The results show very good consistency, especially for aluminum and copper where the specimens each came from a single bar of the material and were more liable to be uniform in structure. Due to the manner of preparation, the lead specimens were not as uniform, therefore giving more scatter to the data. For example, in Figure 24 the specimen having the lower stress-strain curve (Ph250-28) was one that exhibited uneven flow, see Figure 17. The other specimen (Pb250-27) was of the type having a uniform appearance.

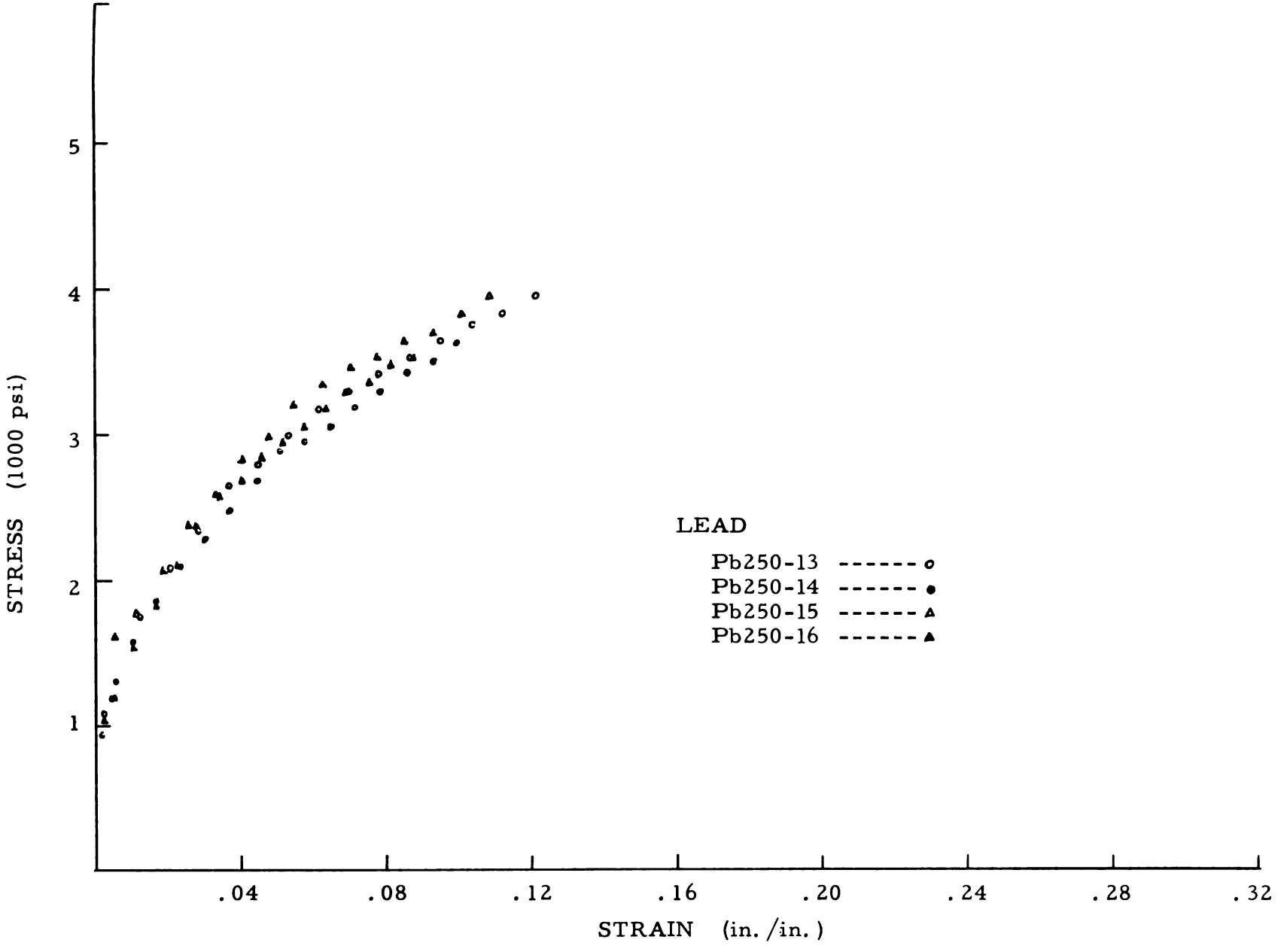

Figure 21. Stress-strain curves for lead at 15 pounds set pressure.

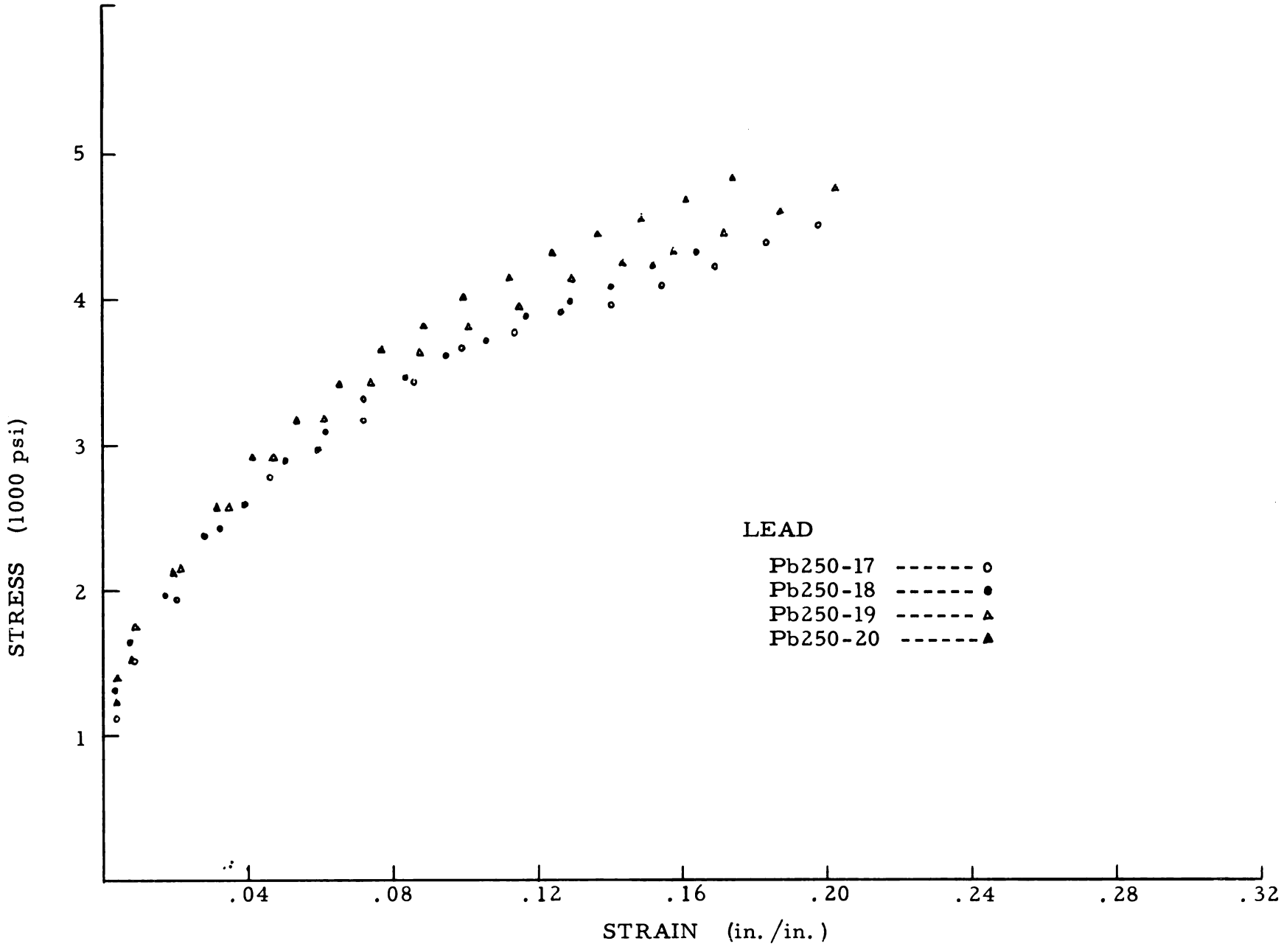

Figure 22. Stress-strain curve for lead at 30 pounds set pressure.

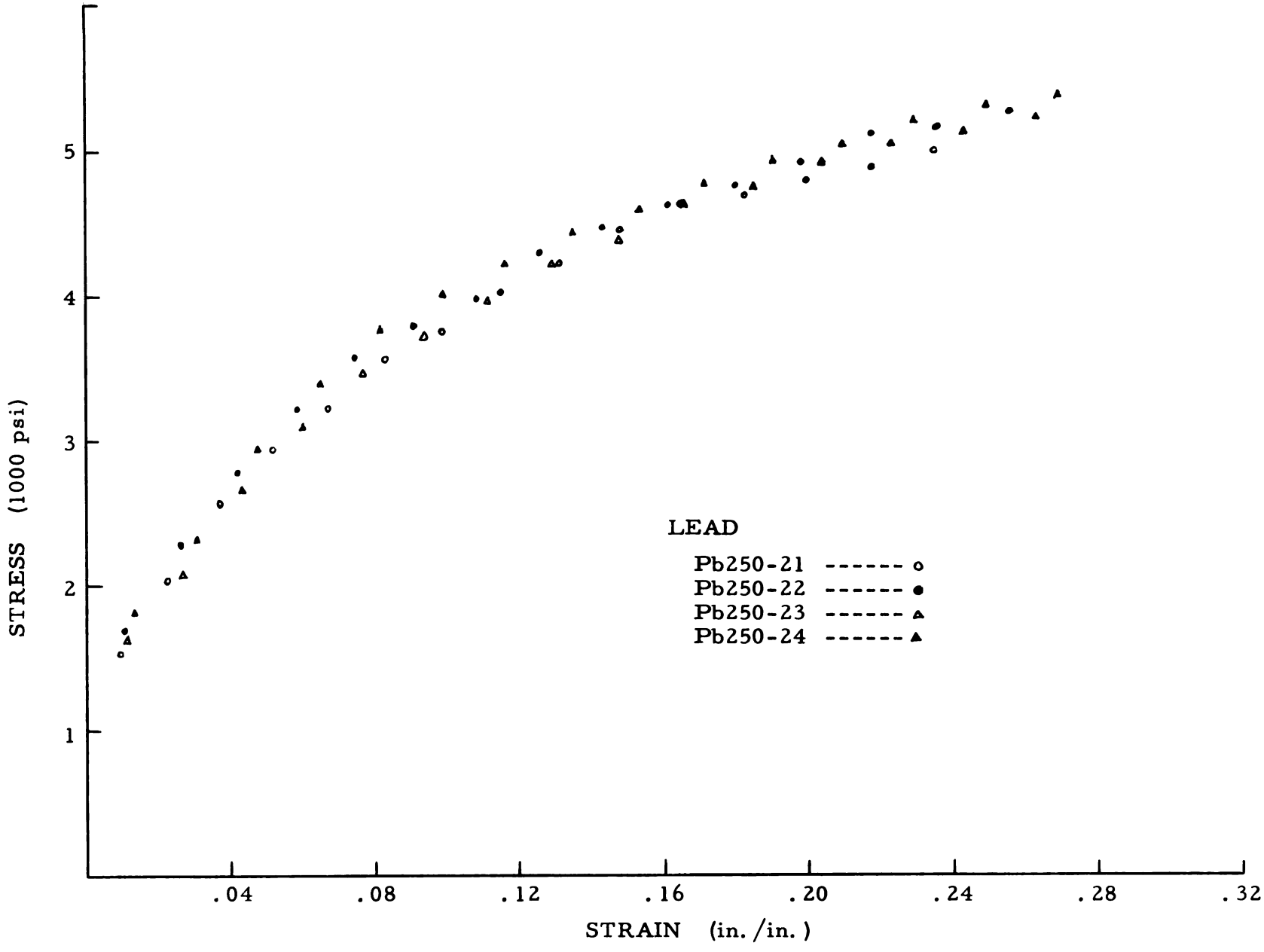

Figure 23. Stress-strain curve for lead at 45 pounds set pressure.

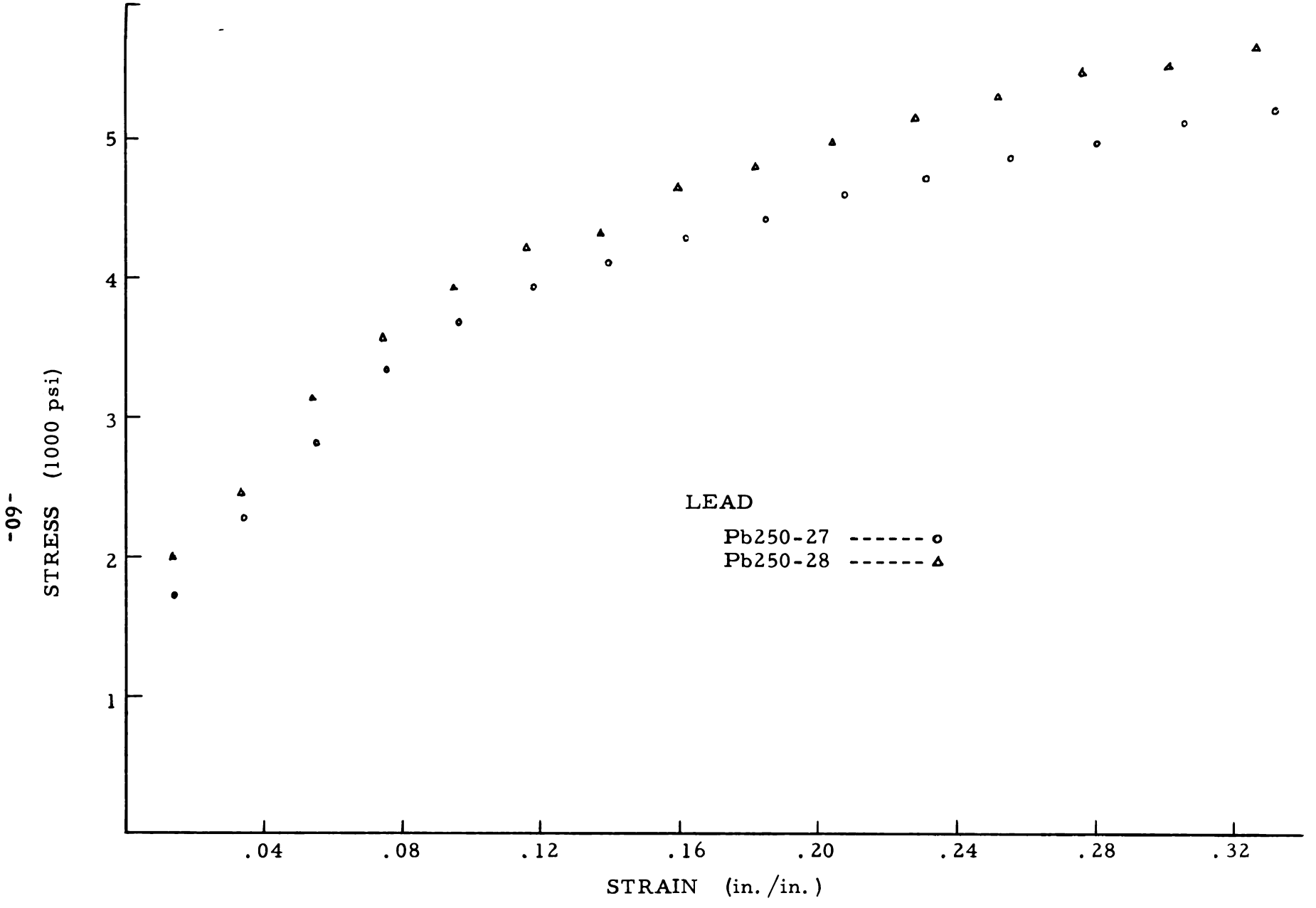

Figure 24. Stress-strain curves for lead at 60 pounds set pressure.

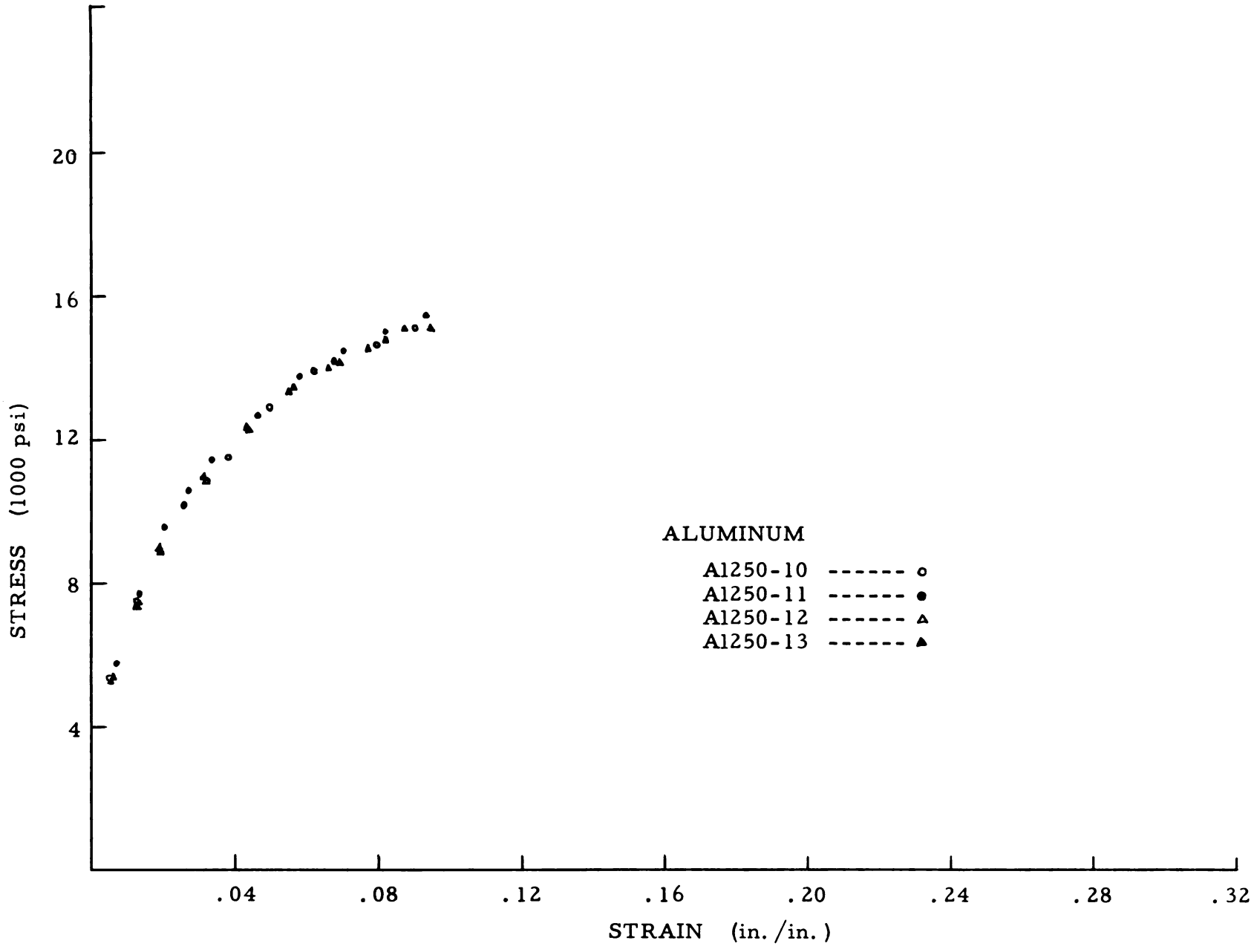

Figure 25. Stress-strain curves for aluminum at 15 pounds set pressure.

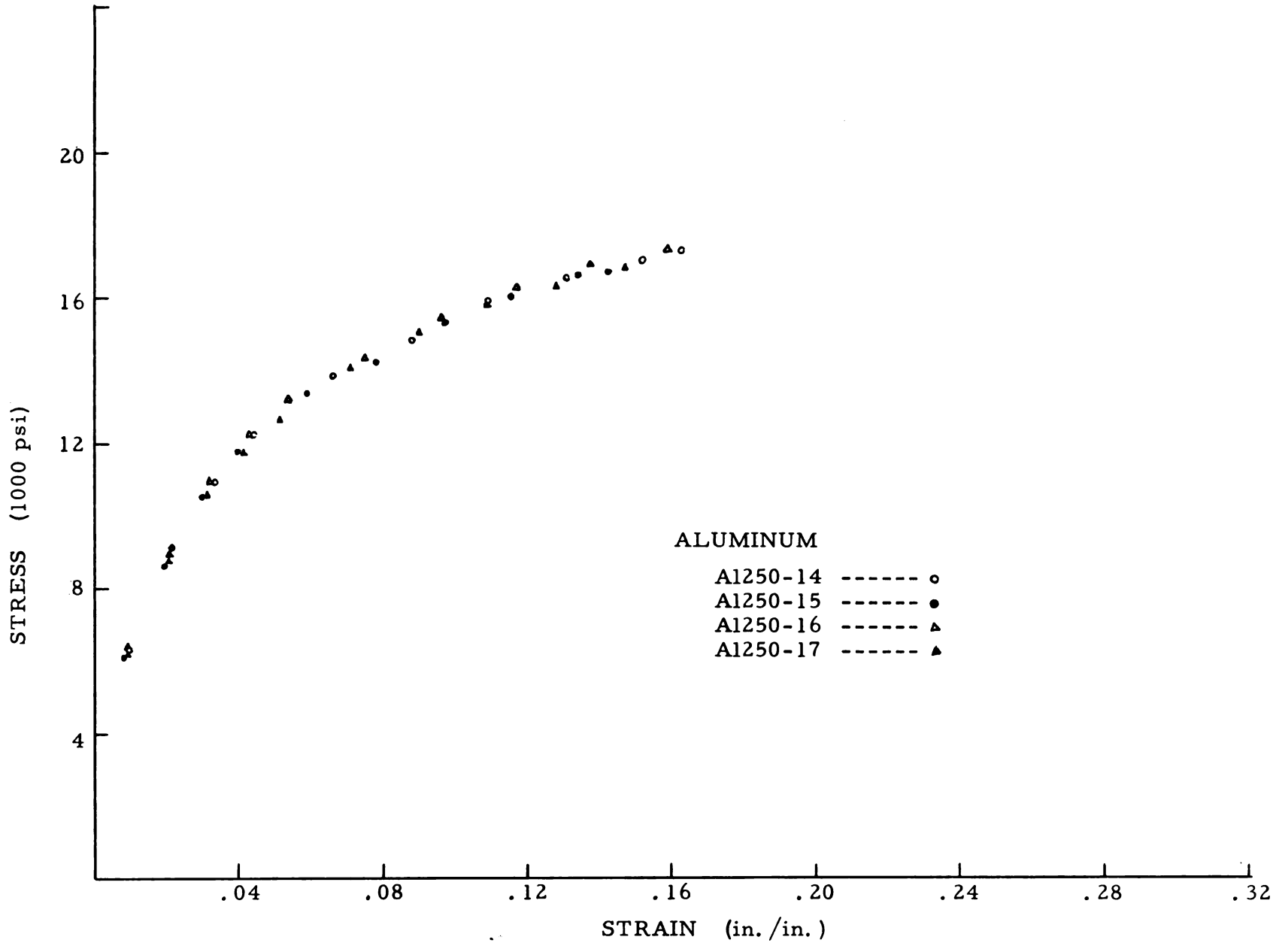

Figure 26. Stress-strain curves for aluminum at 30 pounds set pressure.

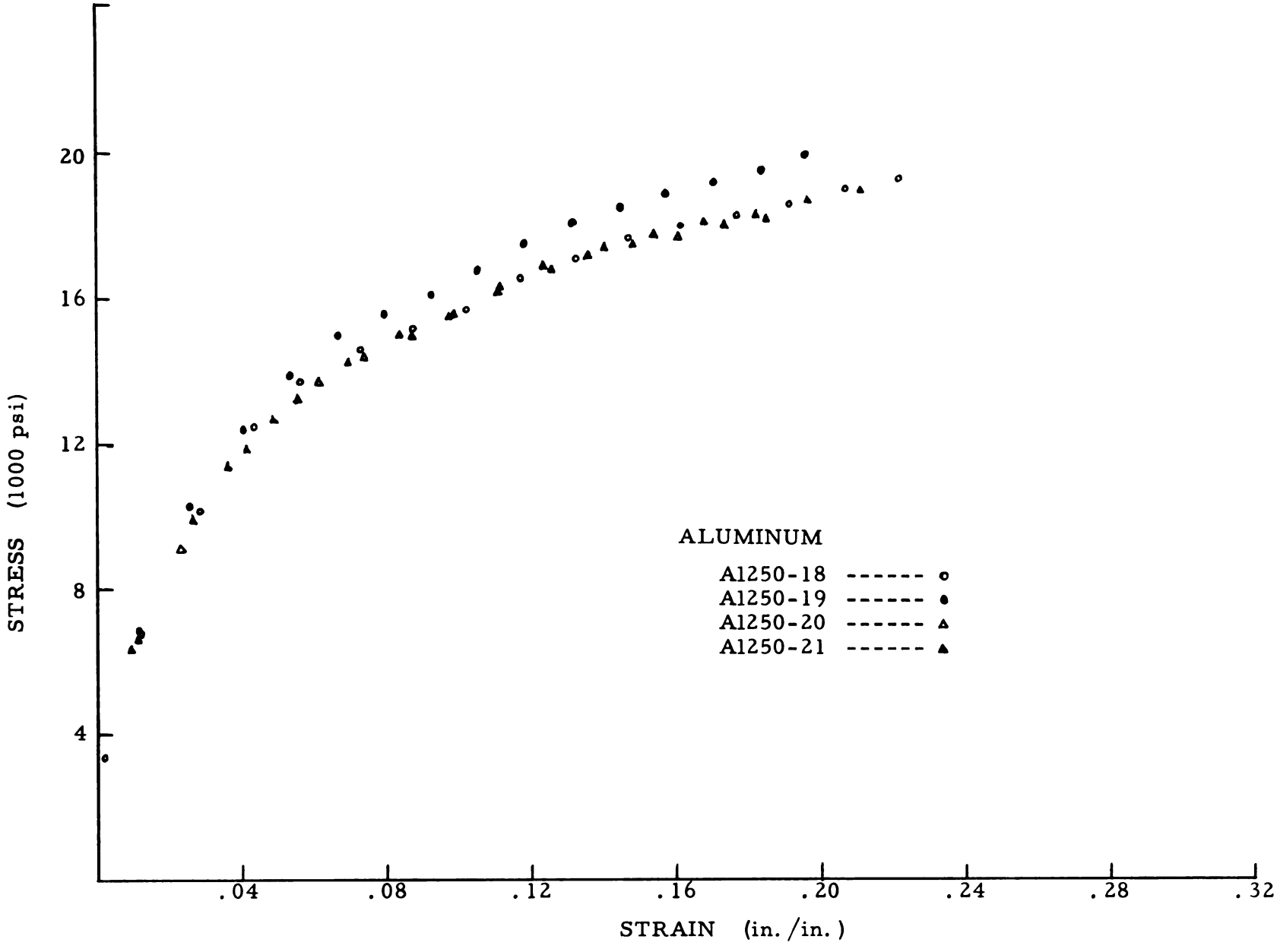

Figure 27. Stress-strain curves for aluminum at 45 pounds set pressure.

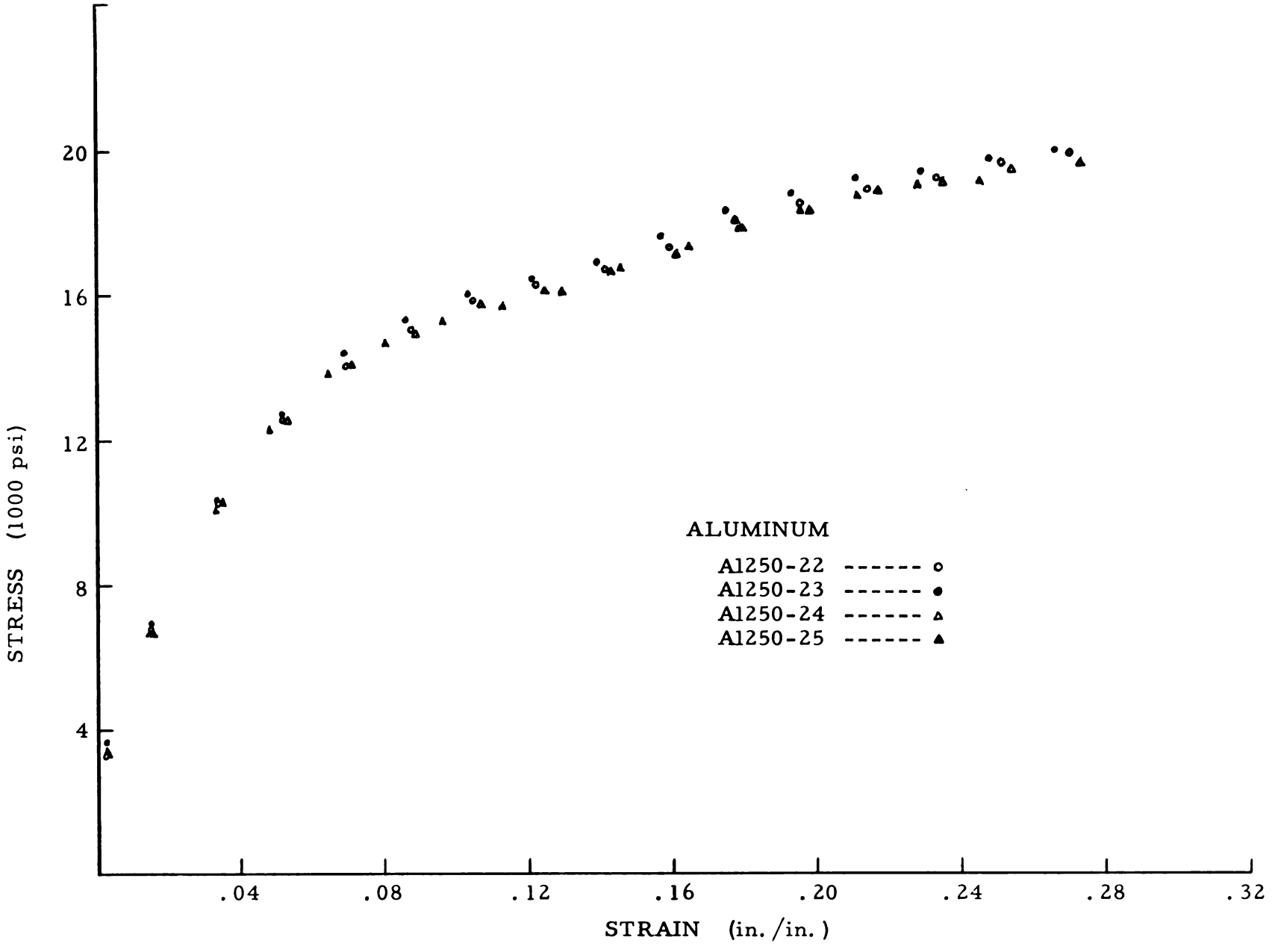

Figure 28. Stress-strain curves for aluminum at 60 pounds set pressure.

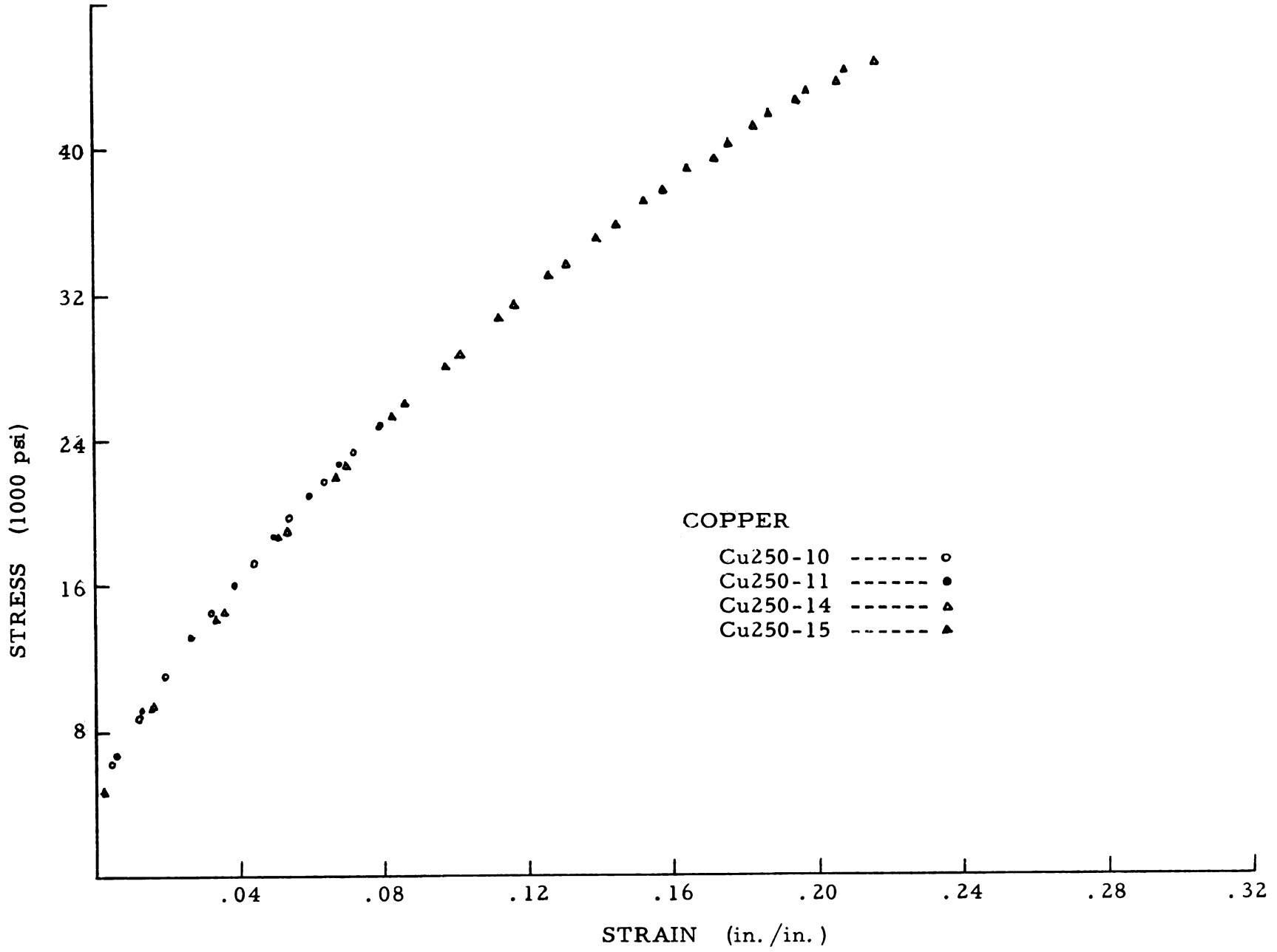

Figure 29. Stress-strain curves for copper at 15 and 60 pounds set pressure.

Over the range of strain rates obtained in these dynamic tests there does not appear to be any significant variation in the stress-strain curves for any of the three metals tested. This may be due to the relatively small variation that should be expected over this limited range in strain rates, as will be seen when the dynamic curves are correlated with those obtained at the lower strain rates. It is also possible, however, that there is an upper or saturation limit on the rate of straining above which the stress required to maintain a given strain remains contant. Such an upper limit has been postulated by Burgers[24] based on the theoretical work of Prandtl[7]. Burgers states that there is a maximum value of stress which a molecular system can sustain. Above this maximum value sliding would be possible at any strain velocity, even if there was no thermal agitation present. However, due to the presence of heat motions, the force necessary for sliding at a finite velocity remains below this maximum. In order to confirm this maximum stress hypothesis, tests at much higher strain rates would have to be performed.

In Figure 30, 31, and 32 an average dynamic stress-strain curve is shown along with average curves obtained at the lower strain rates on the Baldwin testing machine. It is seen that for each metal a homologous set of curves is obtained with an increase in strain rate producing an increase in the stress required to maintain a given strain.

For lead, all of the low strain rate specimens showed deformation of the type having marked flow lines. For this reason in comparing the dynamic with low strain rate behavior only the dynamic specimens of this same type were used.

5.5. Stress-Strain Rate Curves

In order to evaluate the validity of the proposed strain rate laws as given in Equation (4), (5), and (6), the stress required to produce

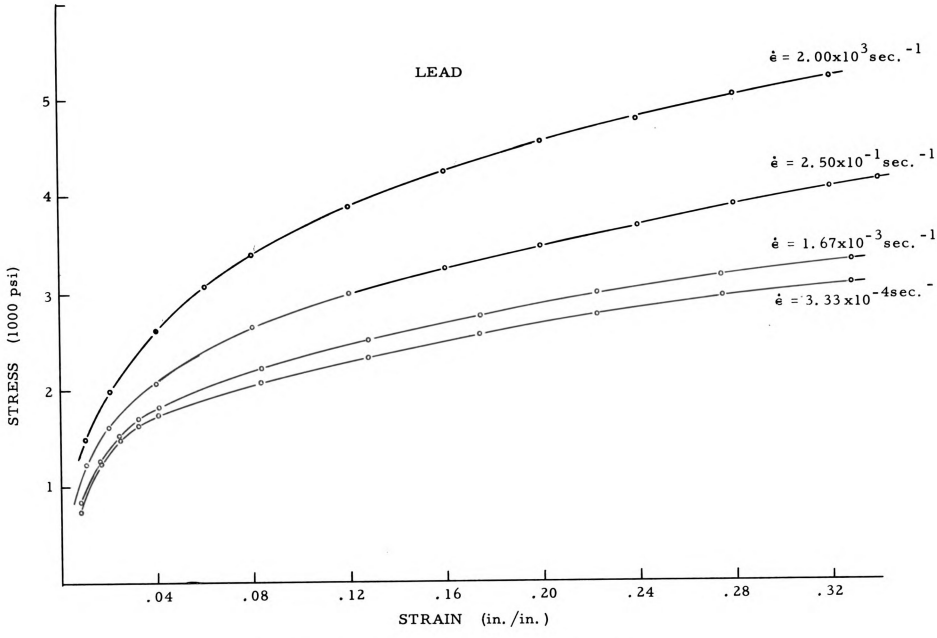

Figure 30. Stress-strain curves for lead at several strain rates.

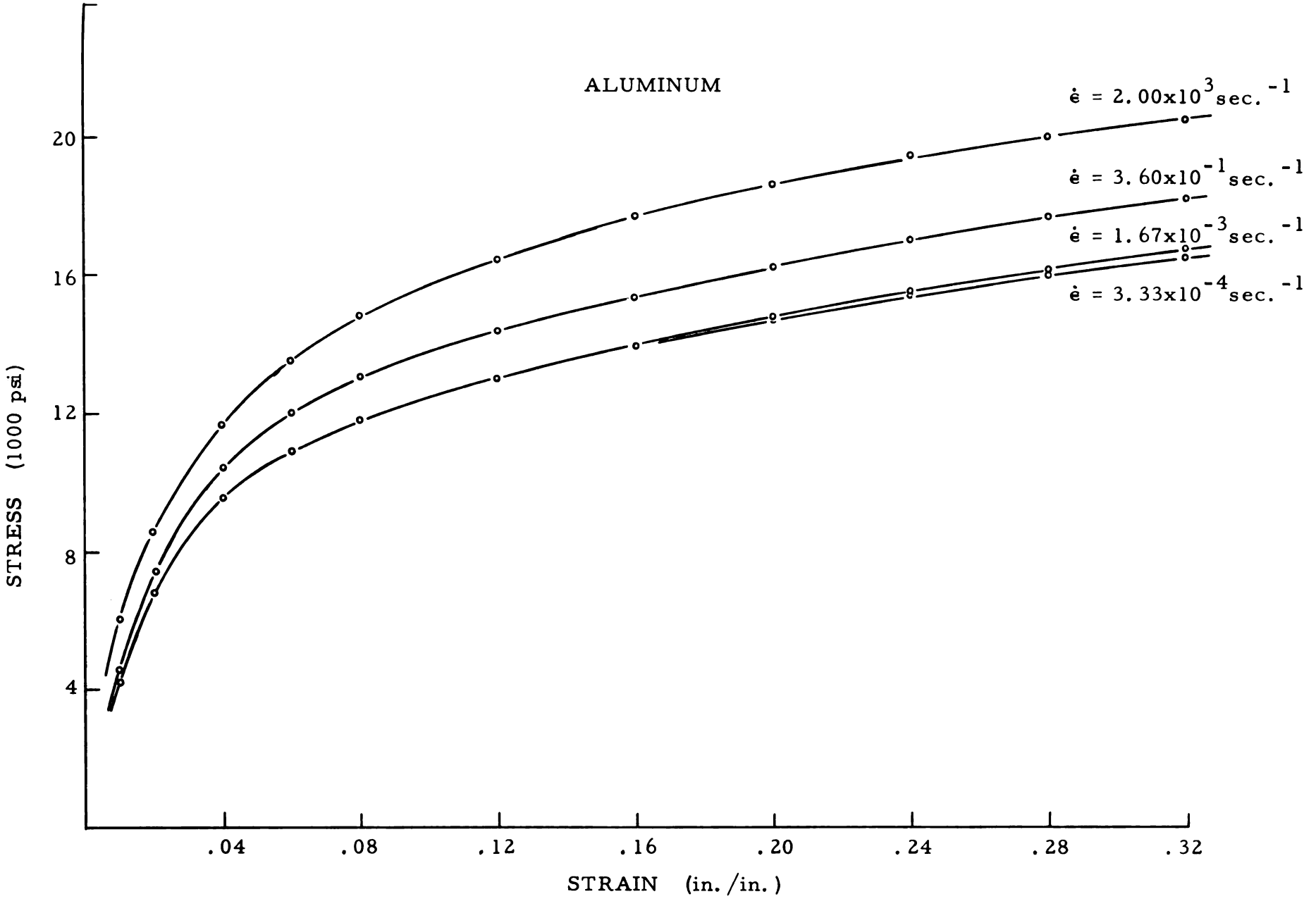

Figure 31. Stress-strain curves for aluminum at several strain rates.

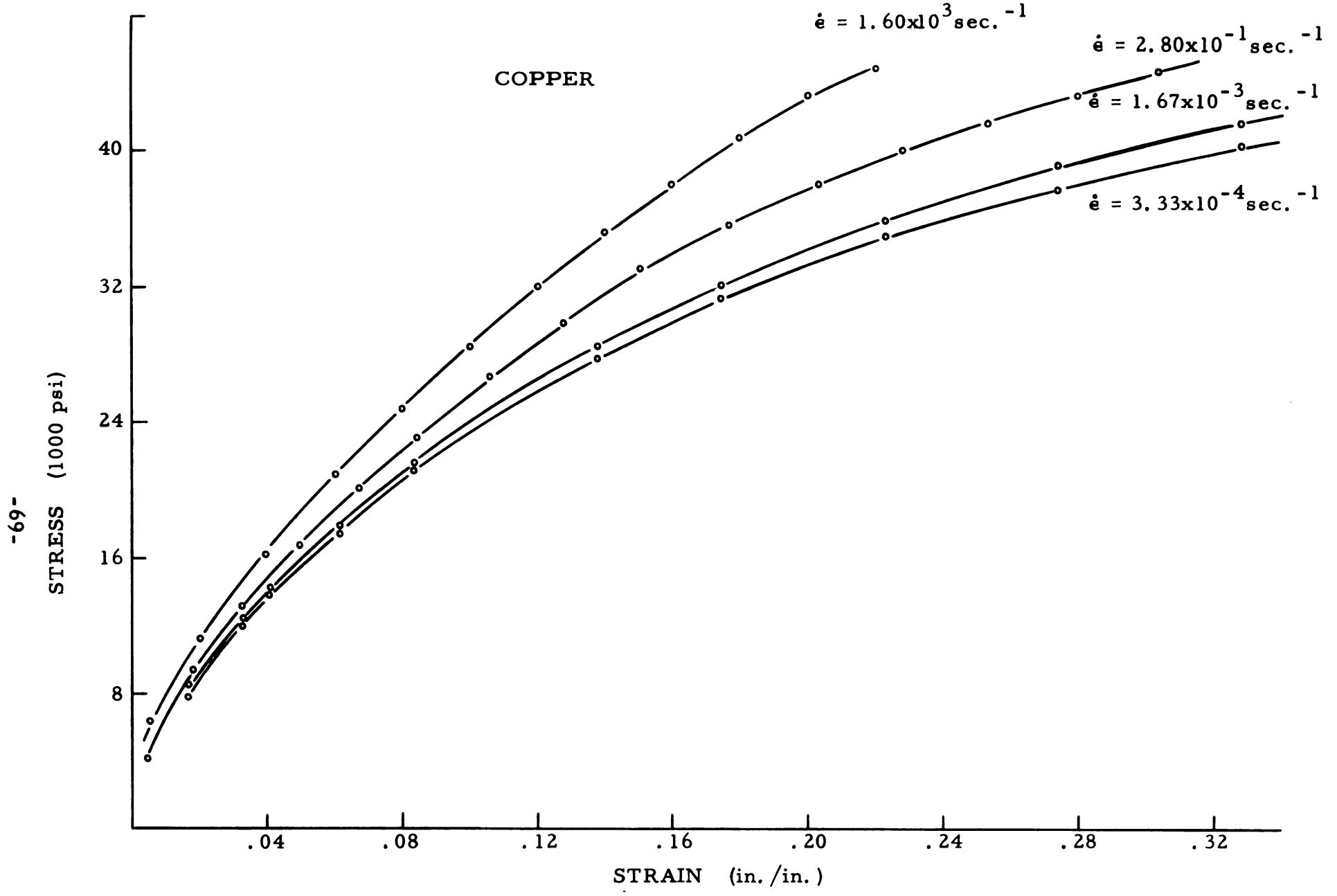

Figure 32. Stress-strain curves for copper at several strain rates.

a given strain was plotted as a function of strain rate for several levels of strain. These curves are given in Figures 33, 34, and 35. For each of the three metals a linear relationship was obtained between stress and the logarithm of the strain rate. In the case of aluminum there is an apparent leveling off at the low strain rates. A similar leveling off might be expected to occur for the other metals if lower strain rates into the creep range were attained. Over the range of strain rates tested, however, the logarithmic law of Equation (5) appears to be valid for lead, aluminum, and copper in the annealed state.

For comparative purposes the results of some other investigators are included in Figures 34 and 35 for aluminum and copper. For aluminum the results of Alder and Phillips[10] show very good agreement with the data of the present investigation. Their results were obtained on compression specimens made from as-extruded aluminum rod and were annealed for one hour at 400°C in vacuum. Results are given for 10 and 20 per cent strain. There is less strain rate effect evident in the results from Alder and Phillips for copper than is indicated by the slope of the data from these tests. Better agreement for copper is obtained with the results from Nadai and Manjoine[18] for ultimate stress vs. log strain rate. Although the effect of strain rate seems to be the same, as evidenced by the comparable slopes in Figure 35, the results of Nadai and Manjoine are not strictly comparable. Their data is for the maximum true stress attained in a tension test as a function of the average strain rate at which the test was run. Since the strain at which the ultimate stress is reached may vary with strain rate, the stress values are not at a constant strain as in the present tests. The specimens of Alder

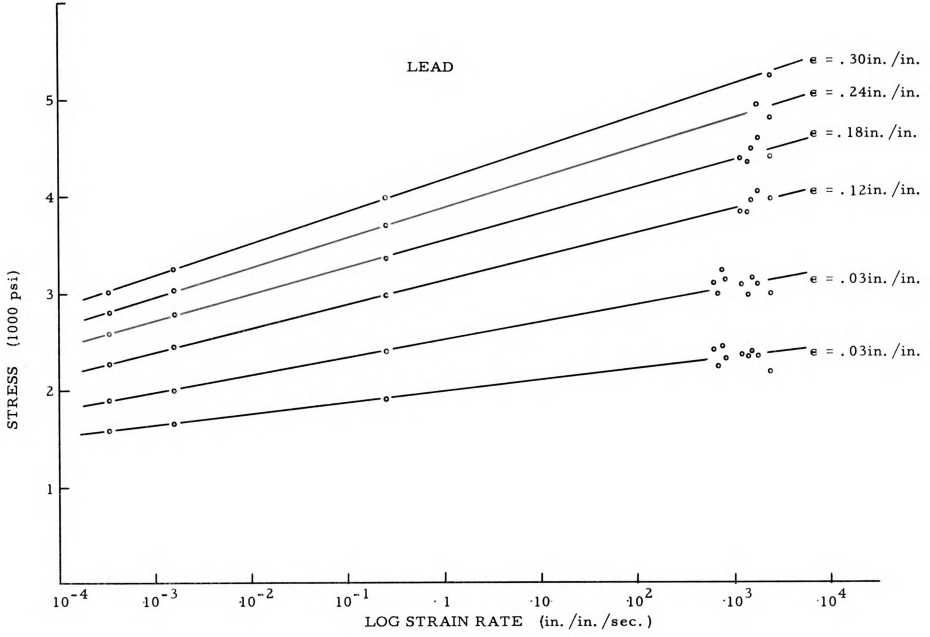

Figure 33. Stress vs. log strain rate for lead at several levels of strain.

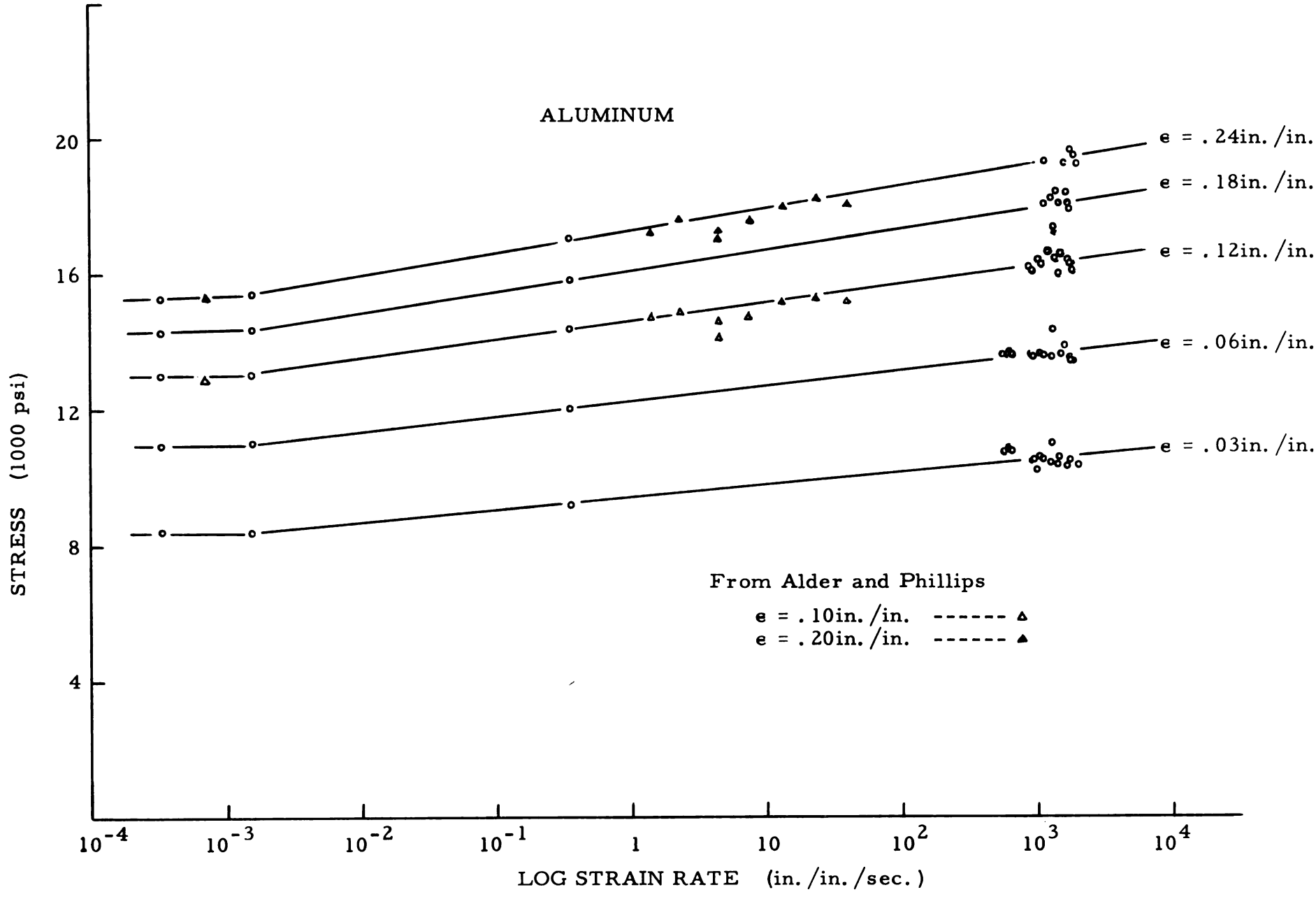

Figure 34. Stress vs. log strain rate for aluminum at several levels of strain.

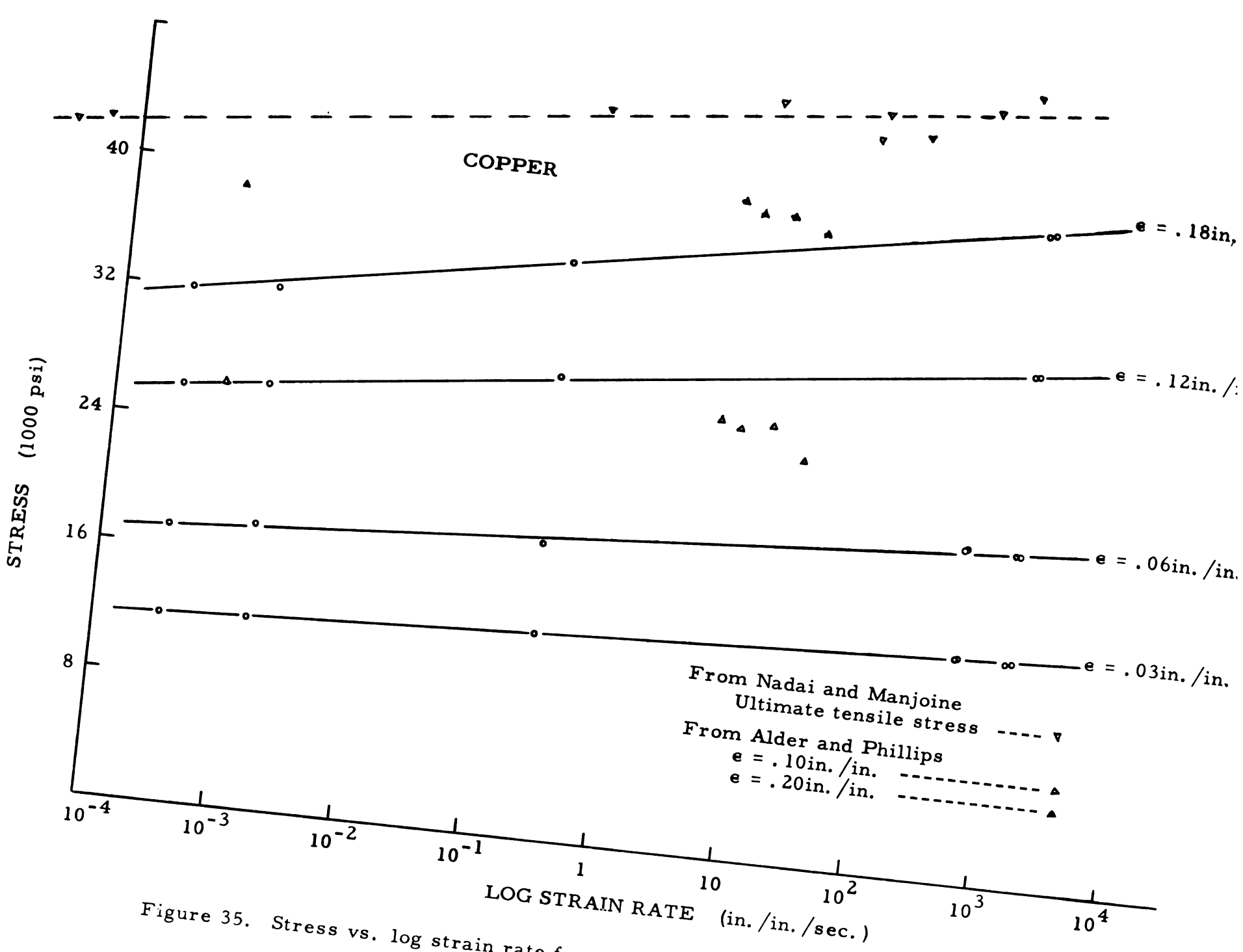

Figure 35. Stress vs. log strain rate for copper at several levels of

and Philips were cold-drawn phosphorous-deoxidized copper, annealed for 2 hours at 600°C in vacuum. Those of Nadai and Manjoine were commercially pure cooper, annealed to 500°C in 5 hours in regenerated gas. The stress values in all cases are true stress.

From Figures 33, 34, and 35 it may be seen that σ_o, the stress at unit strain rate, and k, the constant slope of the stress-log strain rate curves, are functions of strain. Thus Equation (5) may be written

$$\sigma = \sigma_o(\epsilon) + k(\epsilon) \log \dot{\epsilon} . \qquad (25)$$

In this equation $\sigma_o(\epsilon)$ is the stress-strain curve at unit strain rate. The significance of $k(\epsilon)$ may best be visualized by looking at the tangent modulus $\frac{d\sigma}{d\epsilon}$. This is given by

$$\frac{d\sigma}{d\epsilon} = \frac{d\sigma_o(\epsilon)}{d\epsilon} + \frac{d\,k(\epsilon)}{d\epsilon} \log \dot{\epsilon} .$$

Thus, at a given strain, the change in the tangent modulus with strain rate is dependent upon the gradient of $k(\epsilon)$ at the strain. If $k(\epsilon)$ is a constant there is no change in the tangent modulus. For $k(\epsilon)$ an increasing function, an increase in strain rate will produce an increase in the tangent modulus. On the other hand, if $k(\epsilon)$ is a decreasing function, an increase in the strain rate will produce a decrease in the tangent modulus. Up to the highest level of strain achieved in these tests, $k(\epsilon)$ is a monotonically increasing function. Hence an increase in strain rate produced an increase in the tangent modulus for all values of strain.

The increase in the tangent modulus can be associated (see

reference 25) with recovery processes that take place within the deformed structure. Due to the fact that the energy content of the deformed crystal lattice is greater than in the undeformed state, it will be in an unstable condition. The excess energy of the deformed state is gradually dissipated by the movement of unstable particles into positions of equilibrium. The rate of this movement or recovery will be dependent upon both time and temperature such that the extent of recovery will increase with both an increase in time and an increase in temperature.

Another factor influencing the shape of the stress-strain curve is the change from isothermal to adiabatic conditions as the rate of deformation is increased. At high rates of straining the heat produced by the process of inelastic deformation does not have time to be dissipated, thus causing a local increase in temperature. Nadai and Manjoine[18] have measured with thermocouples the increase in temperature of pure iron tensile impact specimens for which the test duration was less than 0.002 seconds. At the point of fracture the temperature increase was found to be about 50°C. Away from the fracture surface the temperature increase was found to be less than half this value. Such an increase in temperature will increase the rate of recovery and should thus tend to flatten out the stress-strain curves at high strain rates. No evidence of such a flattening out was indicated in the present tests, thus the time factor was dominant over any increase in temperature that may have occurred during the tests.

Values for σ_o and k at several values of ϵ are given in Tables 1,

2, and 3 for lead, aluminum and copper. By interpolating between these values and using Equation (25), stress-strain curves may be constructed for any strain rate at which the logarithmic law is assumed to be valid.

Equation (25) may be put in non-dimensional form by dividing through by $\sigma_o(\epsilon)$. Thus,

$$\frac{\sigma}{\sigma_o} = 1 + \frac{k(\epsilon)}{\sigma_o} \log \dot{\epsilon} \quad . \tag{26}$$

Values for k/σ_o are also given in Tables 1, 2, and 3. In Equation (26), the coefficient of $\log \dot{\epsilon}$ is a measure of the rate sensitivity of the material. The larger this coefficient, the greater will be the change in stress for a given change in the rate of straining at any value of strain. From the values of k/σ_o it is seen that lead is more sensitive to rate effects than the aluminum or copper. It is interesting to note that copper is less rate sensitive than aluminum at strains below 12 per cent but is more sensitive at strains above this value. It is also interesting that for aluminum this coefficient is almost constant.

In general practice it may be more useful to take the reference curve $\sigma_o(\epsilon)$ as the normal static stress-strain curve, $\sigma_s(\epsilon)$. Then the increase in stress for an increase in strain rate would be proportional to the difference $(\log \dot{\epsilon} - \log \dot{\epsilon}_s)$, where $\dot{\epsilon}_s$ is the strain rate of the static test. If, for example, we take k/σ_o as 0.05 and $\dot{\epsilon}_s$ as 10^{-4} in./in./sec., then the stress at a strain rate of 10^2 in./in./sec. would be $1.30\ \sigma_s$.

The logarithmic law as first derived by Prandtl was an approximation for large values of stress of the more general law

$$\frac{d\epsilon}{dt} = C \sinh \alpha\sigma \tag{27}$$

TABLE 1. Values of σ_o, k, and k/σ_o for lead.

ϵ	σ_o (psi)	k $(\frac{psi}{sec^{-1}})$	k/σ_o (sec)
.03	2000	116	.0580
.06	2530	181	.0715
.12	3240	247	.0762
.18	3550	277	.0780
.24	3890	308	.0792
.30	4180	330	.0789

TABLE 2. Values of σ_o, k, and σ_o/k for aluminum.

ϵ	σ_o (psi)	k $(\frac{psi}{sec^{-1}})$	k/σ_o (sec)
.03	9400	367	.0390
.06	12200	444	.0364
.12	14600	547	.0375
.18	16100	615	.0382
.24	17300	661	.0382

TABLE 3. Values of σ_o, k, and σ_o/k for copper.

ϵ	σ_o (psi)	k $(\frac{psi}{sec^{-1}})$	k/σ_o (sec)
.03	13000	364	.0280
.06	19200	558	.0291
.12	29100	1081	.0371
.18	36600	1615	.0441

where C and α are dependent on the temperature and the structure. Prandtl's original derivation was based on a molecular model of the dislocation process of the sliding of one row of molecules on another. The hyperbolic sine relation of Equation (27) has also been derived by Eyring[26] from a general equation for the rate of any process where matter rearranges by overcoming a potential barrier, and has since been shown by Nadai[27] to give a good fit to the data of creep tests. The hyperbolic sine or the logarithmic law may thus be valid for many materials over a wide range of strain rates.

6. SUMMARY AND CONCLUSIONS

Dynamic stress-strain curves were obtained for lead, aluminum, and copper using a modification of the method of Kolsky whereby short compression specimens are compressed between two sections of a Hopkinson pressure bar. By using long flat topped loading pulses, uniform strain rates were obtained for a range of strains between 3 and 30 per cent. The elastic portion of the stress-strain curve was not accurately determined. A limitation of the method is that it is not possible to attain as wide a range in strain rates as would be desirable.

Stress-strain curves at constant strain rate were also obtained over a range of rates on a standard testing machine. These results were then correlated with the dynamic tests.

The stress required to product a given strain was found to follow the logarithmic law of Prandtl,

$$\sigma = \sigma_o + k \log \dot{\epsilon}$$

where σ_o and k are functions of strain. The coefficient k determines

the rate of change of the tangent modulus due to a change in strain rate. k/σ_o is a measure of the rate sensitivity of the material.

The tangent modulus increased with an increase in the rate of straining for all three metals tested.

Theoretical basis for the logarithmic form of the rate dependence can be made either from a mechanical model of the dislocation process or from thermodynamical considerations of a rate process.

Further investigations are indicated along several lines: (1) Increasing the range of constant strain rates obtained in the dynamic tests. First, in order to fill in the gap between rates attainable on a standard testing machine and the rates achieved in the present tests, and second, to check whether the stess-log strain rate curve levels off and reaches a maximum value of stress that may be sustained by the material. (2) Obtain constant strainrate tests in the elastic region in order to determind the dynamic modulus of elasticity and yield point. (3) Compare the effect of dynamic strain hardening with static strain hardening. (4) Include the third variable, temperature, in dynamic tests.

7. BIBLIOGRAPHY

1. T. von Karman and P. E. Duwez, "The Propagation of Plastic Deformation in Solids," J. Appl. Phys., vol. 21, 1950, pp. 987-994.

2. G. I. Taylor, "The Plastic Wave in a Wire Extended by Impact Load," The Scientific Papers of Sir Geoffrey Taylor, Cambridge Univ. Press, 1958, p. 467.

3. L. H. Donnell, "Longitudinal Wave Transmission and Impact," Trans. ASME, vol. 52, 1930, pp. 153-167.

4. P. E. Duwez and D. S. Clark, "An Experimental Study of the Propagation of Plastic Deformation under Conditions of Longitudinal Impact," Proc. ASTM, vol. 47, 1947, p. 502.

5. L. E. Malvern, "The Propagation of Longitudinal Waves of Plastic Deformation in a Bar Exhibiting a Strain Rate Effect," J. Appl. Mech., vol. 18, no. 2, 1951, p. 203.

6. E. J. Sternglass and D. A. Stuart, "An Experimental Study of the Propagation of Transient Longitudinal Deformations in Elastoplastic Media," Trans. ASME, vol. 75, 1953, p. 427.

7. L. Prandtl, "Ein Gedankenmodell zur Kinetischen Theorie der Festen Korper," Zeitschrift fur Angewandte Mathematik und Mechanik, vol. 8, 1928, p. 85.

8. P. Ludwik, "Uber den Einfluss der Deformationgeschwindigheit bei Bleibenden Deformationen mit Besonderer Beruecksichtigung der Nachwirkungserscheinungen," Physikalische Zeitschrift, vol. 10, 1909, p. 411.

9. H. Deutler, "Experimentelle Untersuchen uber die Abhangigkeit der Zugspannungen von Verformungsgeschwindigkeit," Physikalische Zeitschrift, vol. 33, 1932, p. 247.

10. J. F. Alder and V. A. Phillips, "The Effect of Strain Rate and Temperature on the Resistance of Aluminum, Copper, and Steel to Compression," J. Inst. of Metals, vol. 83, 1954-55, p. 80.

11. B. Hopkinson, "A Method of Measuring the Pressure Produced in the Detonation of High Explosives or by the Impact of Bullets," Phil. Trans. Roy. Soc. Lond., Ser. A, vol. 213, 1914, p. 437.

12. R. M. Davies, "A Critical Study of the Hopkinson Pressure Bar," Phil. Trans. Roy. Soc. Long., Ser. A, vol. 240, 1948, p. 375.

13. H. Kolsky, "An Investigation of the Mechanical Properties of Materials at Very High Rates of Loading," Proc. Phys. Soc. Lond., vol. 62B, 1949, p. 676.

14. E. T. Habib, "A Method of Making High-Speed Compression Tests on Small Copper Cylinders," J. Appl. Mech., vol. 15, no. 3, 1948, p. 248.

15. E. H. Lee and H. Wolf, "Plastic-Wave Propagation Effects in High-Speed Testing," Trans. ASME, vol. 73, 1951, p. 379.

16. J. W. Turnbow and E. A. Ripperger, "Strain Rate Effects on Stress-Strain Characteristics of Aluminum and Copper," Proc. Fourth Midwest Conf. on Solid Mechanics, Austin Texas Univ. Press, 1959, p. 415.

17. M. Manjoine and A. Nadai, "High Speed Tension Tests at Elevated Temperatures," Proc. ASTM, vol. 40, 1940, p. 822.

18. A. Nadai and M. Manjoine, "High Speed Tension Tests at Elevated Temperatures - Parts II and III," Trans. ASME, vol. 63, 1941, p. A77.

19. M. Manjoine, "Influence of Rate of Strain and Temperature on Yield Stresses of Mild Steel," J. Appl. Mech., vol. 11, no. 4, 1944, p. A211.

20. D. S. Clark and P. E. Duwez, "Discussion of the Forces Acting in Tension Impace Tests of Materials," J. Appl. Mech., vol. 15, 1948, p. 243.

21. D. S. Clark and P. E. Duwez, "The Influence of Strain Rate on Some Tensile Properties of Steel," Proc. ASTM, vol, 50, no. 3, 1950, p. 560.

22. W. R. Campbell, "The Determination of Dynamic Stress-Strain Curves from Strain Waves in Long Bars," Proc. SESA, vol. 10, no. 1, 1952, p. 113.

23. J. E. Johnson, D. S. Wood, and D. S. Clark, "Dynamic Stress-Strain Relations for Annealed 2S Aluminum under Compression Impact," J. Appl. Mech., vol. 20, 1953, p. 523.

24. J. M. Burgers, "Mechanical Considerations - Model Systems - Phenomenological Theories of Relaxation and of Viscosity," First Report on Viscosity and Plasticity, Amsterdam Acadamy of Sciences, Amsterdam, 1935, p. 5.

25. A. M. Freudenthal, The Inelastic Behavior of Engineering Materials and Structures, John Wiley and Sons, Inc., New York, 1950.

26. H. Eyring, "Viscosity, Plasticity, and Diffusion as Examples of Absolute Reaction Rates," J. Chemical Physics, vol. 4, 1936, p. 283.

27. A. Nadai, "The Influence of Time upon Creep. The Hyperbolic Sine Creep Law," Stephen Timoshenko Sixtieth Anniversary Volume, Mac-Millan, New York, 1938, p. 155.

ROOM USE ONLY

APR 19 1962 M

ROOM USE ONLY